



Degree Project in Vehicle Engineering

Second cycle, 30 credits

**Workflow development: study of the influence
of an entire pedaling cycle on the stresses of
an eBike motor, considering triaxial forces and
electric assistance**

THIBAUT JACOB

Abstract

This work aims to develop an alternative working method, implemented to analyse the mechanical strength of an eBike electric motor. It also presents a comprehensive analysis of the influence of a complete pedaling cycle, on the stress state of an eBike motor: the drive unit. In contrast to conventional norm tests based on static or simplified load conditions, the proposed approach considers the full temporal variability of the loads induced by the cyclist's pedaling dynamics, considering also the induced stresses of the electric assistance on the motor. The study emphasizes the effects of considering triaxial stress states during electric motor operation, with respect to the 1D force standard tests conducted so far by BOSCH eBike, evaluating how significant triaxiality is in practice. Furthermore, it consists of developing an automated workflow corresponding to an in-house norm standard test, applicable and adaptable to all BOSCH electric motors.

To address this, the workflow which is developed integrates real-life load cycle data treatment, finite element stress analysis thanks to the software Abaqus, Abaqus subroutines creation and use. A significant part of the study is also devoted to the complete automation of the work routine. The methodology enables the identification of critical stress regions and provides a map of the stresses on the drive unit throughout the realistic pedaling cycle. In addition, it makes it possible to identify the main sources of stress on the electric motor and to conclude that ISO standard tests are more conservative than the tests performed in the scope of this study: triaxiality of pedal forces and electric assistance induced forces have a limited impact on the drive unit in the case of this work.

Keywords

Drive unit, triaxial stresses, finite element analysis, pedaling cycle, mechanical strength, simulation, automation, Python, FORTRAN, Shell Script

Sammanfattning

Syftet med detta arbete är att utveckla en alternativ arbetsmetod för att analysera mekanisk hållfasthet hos en elmotor i en elcykel. Arbetet presenterar också en omfattande analys av hur en fullständig trampcykel påverkar belastningen på en elcykelmotor: drivenheten. Till skillnad från konventionella normtest baserade på statiska eller förenklade belastningsförhållanden, beaktar den föreslagna metoden den fullständiga tidsvariationen hos de belastningar som induceras av cyklistens trampdynamik, med hänsyn tagen även till de inducerade spänningarna från den elektriska assistansen på motorn. Studien betonar effekterna av att beakta triaxiala spänningstillstånd under elmotordrift med avseende på de endimensionella kraftstandardtester som hittills utförts av BOSCH eBike och utvärderar hur betydelsefull triaxialitet är i praktiken. Dessutom består den av att utveckla ett automatiserat arbetsflöde som motsvarar ett internt normstandardtest, som är tillämpligt och anpassningsbart till alla BOSCH-elmotorer.

För att lösa detta integrerar det utvecklade arbetsflödet behandling av verkliga belastningscykeldata, finita element-spänningsanalys tack vare programvaran Abaqus, skapande och användning av Abaqus-subrutiner. En betydande del av studien ägnas också åt fullständig automatisering av arbetsrutinen. Metoden möjliggör identifiering av kritiska spänningsområden och ger en karta över spänningarna på drivenheten under en realistisk trampcykel. Dessutom gör den det möjligt att identifiera de viktigaste källorna till spänningar på elmotorn och dra slutsatsen att ISO-standardtesterna är mer konservativa än de tester som utförts inom ramen för denna studie: triaxialiteten hos pedalkrafterna och de krafter som induceras av den elektriska assistansen har en begränsad inverkan på drivenheten i detta fall.

Nyckelord

Drivenhet, triaxiala spänningar, finita elementanalys, pedalcyklrörelse, motstånd, simulering, automatisering, Python, FORTRAN, Shell Script

Acknowledgments

I would like to express my gratitude to my internship supervisors, Julien Hassler, and to Leo Cretin at BOSCH eBikes, as well as to the entire Drive Unit simulation team, for their continuous support, their availability, and the time they generously dedicated to me. Their technical expertise, valuable advice, and constant good spirit made this internship both an enriching professional experience and a truly enjoyable journey. I am also very thankful to my academic supervisor at KTH Royal Institute of Technology, Lars Drugge, whose guidance, feedback, and encouragement greatly contributed to the success of this work. Finally, I would like to extend my gratitude to my professors at my French engineering school, for their commitment and for providing me with the foundations and mindset necessary to carry out this project. This thesis would not have been possible without the contribution, patience, and kindness of all these people, to whom I am sincerely indebted

List of abbreviations

DU / BDU	Drive unit / Bosch drive unit
FEM / FEA	Finite element method / Finite Element Analysis
BCs	Boundary conditions
ISO	International Organization for Standardization

CONTENTS

1. Introduction.....	1
1.1 BOSCH eBike presentation.....	1
1.2 Context of the study	2
1.3 Object of the study	3
2. Background.....	6
2.1 Preliminary work and resources	6
2.2 Materials - resources.....	6
3. Methods	7
3.1 3D pedaling data.....	7
3.2 Pedaling cycle simulation	10
3.3 Abaqus processing and workflow automation	23
3.4 General summary of the working routine.....	28
4. Results	29
4.1 Standard pedaling cycle analysis	29
4.2 ISO norm test comparison	34
4.3 Workflow documentation – Knowledge transfer.....	39
5. Conclusions.....	40
6. Points of perspective	42
References.....	43
Appendix.....	44

List of Figures

Figure 1. BOSCH SX electric motor (BDU31)	4
Figure 2. Main steps of the thesis work.....	4
Figure 3. BDU31 finite element model used for the study	6
Figure 4. The coordinate reference according to the data acquisition (front of the bike on the left).....	7
Figure 5. Example of a data collected	8
Figure 6. Maximum and minimum occurring pedal forces for all measurements in a radial projection of the crank angle for the right and left crank revolution.....	8
Figure 7. Pedaling cycle segmentation (every 15 degrees)	9
Figure 8. YZ DU cross-section highlighting the bearing bracket (green) and some bearing outer rings (red)	10
Figure 9. Fastening screws (left ones in red and right ones in green)	11
Figure 10. DU force flow chart	12
Figure 11. Shafts and gearing configuration inside the DU (shafts in yellow, gearing in green and bearings in red)	13
Figure 12. Shafts and gearing simplified system	14
Figure 13. Moments induced by X-component of gear interaction force.....	16
Figure 14. Components of helical gears contact force	16
Figure 15. Derivation of components of contact force	17
Figure 16. Forces configuration on the crankshaft (pedal force on the right side only).19	
Figure 17. System simplification of the crankshaft	19
Figure 18. Simplified system including motor induced force and moment	19
Figure 19. Contact configuration between the shaft (white) and the bearing (stripped)	21
Figure 20. Shaft/bearing contact pressure distribution model ((a) uniform pressure distribution model, (b) sinusoidal pressure distribution model, and (c) Hertz pressure distribution model).....	22
Figure 21. Sinusoidal pressure distribution model description.....	22
Figure 22. Abaqus subroutine process	23

Figure 23. Abaqus simulation procedure (input files in orange and output files in green)	23
Figure 24. Both simulation scenarios	24
Figure 25. Step n of the simulation - Stage 1: simulation of the step n.....	25
Figure 26. Step n of the simulation - Stage 2: compiling results of step n with all the previous steps.....	25
Figure 27. Python automation script operating mode.....	26
Figure 28. Shell script automation operating mode	27
Figure 29. Workflow summary: files and software interactions	28
Figure 30. Dataset used for the standard pedaling cycle	29
Figure 31. Simulation results for the angle of 135 degrees (BCs areas circle in red).....	31
Figure 32. DU simulation results (90 degrees)	32
Figure 33. DU simulation results without electric assistance (90 degrees)	33
Figure 34. Crank unit: ISO test with crank arms inclined at 45 degrees to the horizontal (typical test setup).....	34
Figure 35. DU scaled simulation results (90 degrees).....	36
Figure 36. Shafts attachment areas in the DU (scaled pedaling cycle test results)	38

List of Tables

Table 1. Scaled pedaling cycle data for the critical angle (90 degrees) 35

1. Introduction

1.1 BOSCH eBike presentation

1.1.1 BOSCH group

Everything started in 1886, when Robert BOSCH opened a “Workshop for Precision Mechanics and Electrical Engineering” in Stuttgart [1]. This marked the birth of what became a global industrial leader, which stands out for its commitment to innovation and social responsibility. The company’s first major success came in the mid-1890s, when it specialized in precision mechanical and electrical engineering. A turning point was the invention of a magneto ignition system for a stationary engine in 1896. In 1897, BOSCH began equipping automobiles with its reliable ignition system, becoming a leading automotive supplier.

BOSCH’s global growth accelerated in the early 20th century. Despite the disruption of World War I, BOSCH continued to innovate, developing new products like generators, lighting systems, windshield wipers, and horns. In 1918, the company introduced its iconic logo, which remains in use today. During World War II, BOSCH shifted its production to support the war effort but was allowed to continue automotive manufacturing. Some factories were destroyed, but the company recovered by producing spark plugs and cookware. BOSCH also demonstrated its social commitment by helping persecuted Jews avoid deportation or flee abroad.

In the second part of the 20th century, BOSCH expanded in new sectors such as power tools (e.g., hammer drills) and thermotechnologies. In the 1950s, the company launched household appliances, power drills, car radios, and kitchen robots, selling millions of units. In the 1960s–1980s it expanded into electronics, telecommunications, semiconductors, and embedded systems. BOSCH invented the famous technology ABS (Anti-lock Braking System) and developed the lambda sensor (supplies the necessary information for optimal air/fuel mixture to the engine control unit), both automotive industry standards.

Today, the BOSCH group hire more than 410,00 employees worldwide, including 86,300 researchers and engineers. The group produces 90,3 billion € (2024) sales revenue thanks to its 490 subsidiaries and regional companies in some 60 countries.

1.1.2 BOSCH eBike Systems

Part of the BOSCH group, BOSCH eBike Systems was founded as a start-up in 2009 and launched its first eBike drive system in 2010. The company equips the bicycles with a BOSCH system including a drive unit (DU), a battery, a display and the associated software. Their different eBike systems are designed to be versatile and adapt to a wide

range of habits, making eBikes accessible and practical for most people and many different types of use: city biking, cargo biking, mountain biking and so on. At the end of the 2010s, BOSCH eBike established itself as a leader in the eBike market, consistently holding the largest market share in Europe for eBike drive systems (often cited at ca. 50%+ depending on segments and year [2]). Thanks to its success, it became in 2020 a separate business unit within the BOSCH group, on the same level as the automotive and home appliance divisions. Every year, several hundreds of thousands DU are produced by BOSCH eBike, and they are all designed and engineered in the eBike Campus and research centre, in Kusterdingen in Germany, where this Master Thesis has been completed.

1.2 Context of the study

1.2.1 Climate emergency

Even though an ecological awareness is taking shape worldwide, particularly through large-scale organizations actions and projects such as the Intergovernmental Panel on Climate Change (IPCC, the United Nations body responsible for assessing the science related to climate change) researches, the Paris agreements, or the various COPs (Conference of the Parties) held each year, human pressure on the environment remains unsustainable. The efforts made so far are certainly necessary but currently insufficient; whereas the Paris agreements aimed to limit global warming to 2 degrees (above pre-industrial levels) and reach carbon neutrality by 2050, nowadays, despite the efforts of the countries, the goals seem difficult to achieve due to how slowly CO₂ emissions are decreasing. Indeed, global CO₂ emissions have reached historical highs, approaching 40 billion tonnes in 2024 (see [Appendix Figure A-1](#) [3]). The planet is facing an increase in the frequency and intensity of natural disasters, a clear sign of climate disruption. This is not surprising when considering that, 7 out of the 9 planetary boundaries (as illustrated in [Appendix Figure A-2](#) [4]) have already been crossed, threatening more than ever the stability of the Earth's ecosystem.

1.2.2 Transport – Soft mobility as part of the solution

In this context, the transport sector plays a major and problematic role, as it accounts for 24% of global CO₂ emissions (and 34% for France), knowing that about 74% of these emissions come from road vehicles [5]. This is underscoring a strong dependence on carbon-intensive vehicles and lifestyles. But, beyond global warming, transports are also responsible for important urban congestion, noise pollution, deterioration in air quality, resulting in numerous respiratory diseases (emissions from particles, tires, brakes, etc.).

Decarbonization of the transport sector therefore appears to be a necessity, and the introduction of soft mobility (eBikes, electric scooters, public transports, ...) is one of the ways to achieve this. These mobilities are helping to build quieter, healthier cities,

fostering active lifestyles, contributing to a resilient, low-carbon society and reducing car dependency and traffic

1.2.3 BOSCH eBikes: a consistent solution

EBikes products proposed by BOSCH eBike Systems as part of the soft mobility solution, appear as relevant, offering a concrete and accessible alternative to conventional road transports. In this scope of mobility, it is therefore necessary to offer high-quality products that are durable and provide unfailing safety. This is why improving the robustness and safety associated with the use of BOSCH eBikes is a key focus of engineers' research. The aim of this master thesis is therefore to investigate this approach.

1.3 Object of the study

1.3.1 Introduction to the topic

Products on the market like eBikes must respect norms such as ISO norms (International Organization for Standardization) and consequently must pass ISO norm tests, international standardization and security norms which provide frameworks for quality, safety, efficiency and interoperability across industries. To take testing even further, BOSCH wants to conduct its own mechanical strength tests which broaden the previous scopes of study of eBikes by trying to get closer to real-world conditions of use. Indeed, current ISO test for the strength of the DU consists in applying consecutively, a right and a left pedal 1D or 2D force on the system frame/DU [6]. The idea of the new DU test developed jointly with engineers from the DU simulation team, is to test the resistance against stresses, of the DU fixed on the frame under the load of an entire pedaling cycle, considering triaxial forces and the constraints induced by the electric assistance of the motor. This thesis work will only focus on the simulation part and not on real-life testing. Finally, the aim of this study is to develop a workflow whose purpose is to extract real pedaling data, use these 3D forces, motor moments and pedal angles as inputs for FEM simulation tests, observe the reaction of the fixed DU under the constraints and analyse the results through the prism of mechanical strength and user safety. The tests will be operated on the BDU31 (Figure 1), which is the BOSCH SX drive unit, the most compact and lightweight of the DU series, already on the market.



Figure 1. BOSCH SX electric motor (BDU31)

1.3.2 Quick overview of the study process

To provide a quick overview of how this study is conducted, the main stages of the work carried are highlighted in Figure 2:

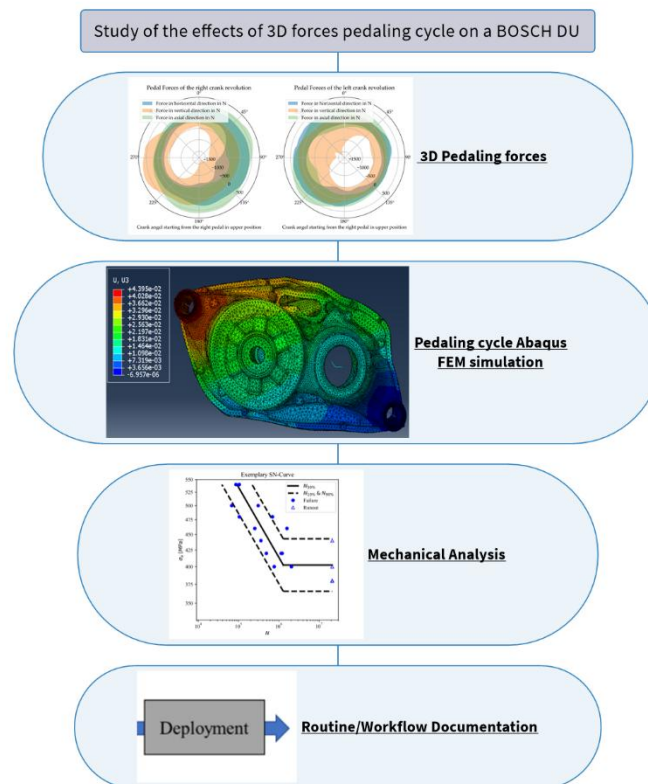


Figure 2. Main steps of the thesis work

1. 3D pedaling forces

Consists in gathering real pedaling data, making them exploitable for the study and selecting those that are relevant to the work.

2. Pedaling cycle Abaqus FEM simulation

Consists in using data collected in real-life situations as inputs for the FEM simulation in the Abaqus software. The use of python language and shell script will be required to automate the task. A part of the work will be allocated to the calculus of the mechanical equilibrium of the considered system, to find the equivalent forces and loads applying on the simulation model. Another part, will be allocated to the FORTRAN dload subroutine, needed for the Abaqus simulation. Everything will be detailed in the following section [3 Method](#).

3. Mechanical analysis

This step aims to analyse the results on the DU, obtained from the simulation: which part is under the most stress? Which pedal angle is the most critical? Are the stresses imposed by electric assistance significant? Is there a risk of damage? What could be the limit input before damages? Are the results far from results of the ISO norm tests?

4. Routine/Workflow deployment

This section ensures the effective transfer of knowledge between the thesis work and the engineers at BOSCH eBike. Indeed, this work must be understandable for every BOSCH eBike simulation engineer so that it can be reused for the upcoming work of the simulation team. A transfer of skills will also be carried out with the next master's thesis student who will take over the task.

2. Background

2.1 Preliminary work and resources

This work follows on from the work of two previous students. At first, pedaling data acquisitions were resumed from the thesis work of the former PhD student Marco Steck [7]. A knowledge transfer was carried out to ensure full understanding of the data provided. In addition to that, the simulation model of the DU used for the upcoming tests (Figure 3), has been adopted from the previous master thesis work of Fanny Ibrahime Malick (Grenoble INP – ENSE3 [8]), because the aim of this study was to focus on the creation of the mechanical strength test (not on the creation of the finite element model itself).

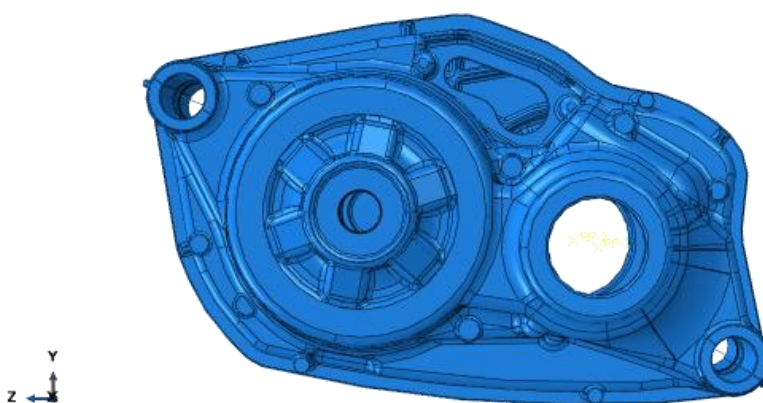


Figure 3. BDU31 finite element model used for the study

The first few days and weeks of work were devoted to studying how the DU simulation team operates, as well as how the DUs themselves operate (particularly the BDU31, which is the subject of the study), and the ISO standards with which they must comply.

2.2 Materials - resources

Since very little specific material is required for the purposes of the study, the liberty of relegating the “Materials” section to this “Background” section has been taken. Indeed, the needed material is the following:

- A laptop
- A python compiler
- The software Abaqus for the FEM simulation
- A virtual machine called HPC to proceed to faster simulations compared to the laptop and its limited computing power and to be able to compile FORTRAN language
- The Office package and diagram creation tools

3. Methods

3.1 3D pedaling data

3.1.1 Pedaling data structure and overview

As mentioned in the previous section, all the data set was already collected by the previous PhD student Marco Steck as .pickle files. A .pickle file is a file used in Python to serialize and deserialize Python objects. In simpler terms, serialization is the process of converting a Python object (e.g. dictionary, custom class instance, etc.) into a byte stream. This byte stream can then be saved to a file, transmitted over a network, or stored in a database. And deserialization is the reverse process of taking that byte stream and reconstructing the original Python object from it. It means that this form of data is easily manipulable with python code, what is interesting in terms of the upcoming complete workflow automation.

The data collected covers all types of scenarios, such as uphill scenarios, downhill scenarios and electric motor off scenarios, etc. It is important to note that the recorded data corresponds to the right pedal in the raised vertical position as the starting angle ($=0^\circ$) of the pedaling cycle. The X, Y, Z coordinates are defined as shown in Figure 4:



Figure 4. The coordinate reference according to the data acquisition (front of the bike on the left)

What do the datasets give access to?

- 3D pedaling forces for both pedals (L and R), according to X, Y and Z [N]: FLX, FRX, FLY, FRY, FLZ, FRZ
- The speed [km/h]: Geschwindigkeit
- The motor moment [Nm]: Motormoment
- Resulting forces on the left (Links) and right (Rechts) pedal [N]: Fres_Links, Fres_Rechts

- The forces in the cylindrical coordinate system [N]: Ftan, Winkel_Z_Links, Winkel_Z_Rechts, Winkel_XY_Links, Winkel_XY_Rechts
- The pedal angle [°]: Kurbelwinkel
- The number of the test drive and the number of pedaling cycle, within the acquisition: Messfahrt, Kurbelcyclus

Figure 5 is an example of a data set, .pickle file processed with Python (table cut because it was not possible to display all the parameters at the same time):

Index	Kurbelwinkel	Ftan	FRZ	FLZ	Motormoment	eschwindigkeit	FXR	FYR	FXL	FYL	Messfahrt	Kurbelzyklus
0	146	20.7	6.3	-51.2	1587	7.4	-64.1604	-65.1093	-26.8684	-83.3793	1	0
1	147	22.8	19.4	-60.3	1555	7.4	-49.6427	-86.9679	-15.3801	-97.8651	1	0
2	148	16.6	33.4	-51.6	1531	7.4	-33.7276	-96.4248	-23.6244	-81.2678	1	0
3	149	22.1	18	-49.9	1508	7.5	-51.0411	-76.4006	-23.3421	-79.5901	1	0
4	150	14.8	28.8	-49.4	1480	7.5	-30.5404	-91.3024	-20.8733	-78.4465	1	0

Figure 5. Example of a data collected

However, the only information needed for the rest of the study are the 3D pedaling forces and the motor torque, according to the pedal angle, because they are responsible for the stresses, studied inside the DU. It is easy to imagine why pedal forces are responsible for stresses in the DU, but later subsequent discussion will address how the motor torque also contributes to stresses in the DU.

To get an idea of the magnitude of the forces exerted on the pedals during the use of an eBike, Figure 6 is summarizing the measurements taken from [7]:

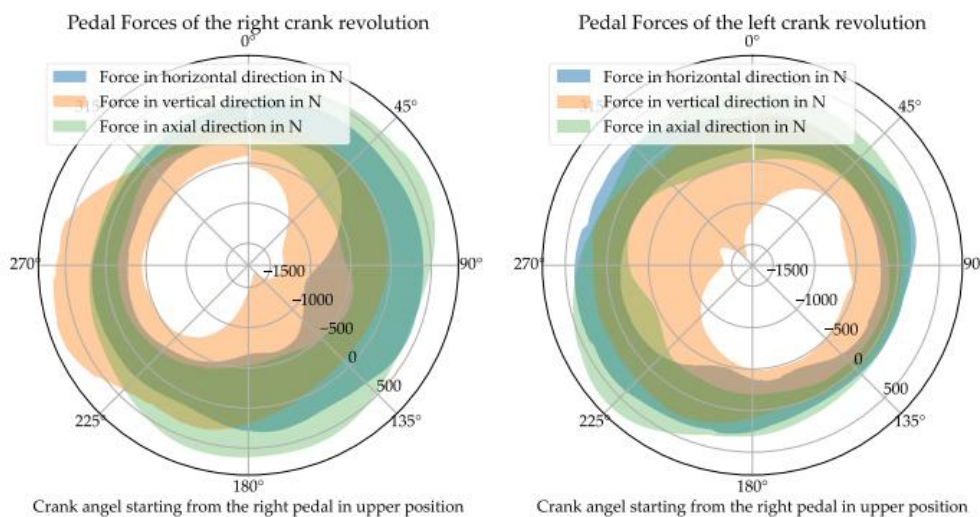


Figure 6. Maximum and minimum occurring pedal forces for all measurements in a radial projection of the crank angle for the right and left crank revolution

3.1.2 Focused dataset of the study

There is a large amount of data; for the purposes of the study, it is necessary to reduce the scope of the data to be studied. The considered dataset as starting point of the study must be large enough for the study to be accurate, but not too large so that the quantity of treated information and the calculation time do not become excessive. As agreed with the BOSCH DU simulation team, the idea is to be able to perform a quick simulation (<1-2 hour) while having a rough idea of the angle range of the pedaling cycle for which the DU is experiencing the highest mechanical stresses. The aim is to run a simulation containing different steps each representing a pedal angle of the pedaling cycle. The choice of sampling rate for the pedaling cycle remains crucial.

Realizing the simulation with a step each degree of the pedaling cycle (360 data point for the 360 degrees of the cycle), would give a really accurate mapping of the DU stresses during the pedaling cycle, but would also need 360 Abaqus simulation steps. So, with the DU simulation team; the arbitrarily chosen idea would be to use a data set with a point every 15 degrees: a 24 points data set. Intervals of 15 degrees are considered because ISO norm tests are also using multiples of 15 degrees for their pedal angle test configuration. The results of the mechanical study will give a general idea of the maximum stresses inside the DU during the pedaling cycle and if greater precision is required, it will be possible to refine the dataset in the relevant angle area.

Figure 7 is detailing how the pedaling cycle is sampled. Each red dot represents a point in the considered dataset for the study and will be used as one step in the entire pedaling cycle simulation:

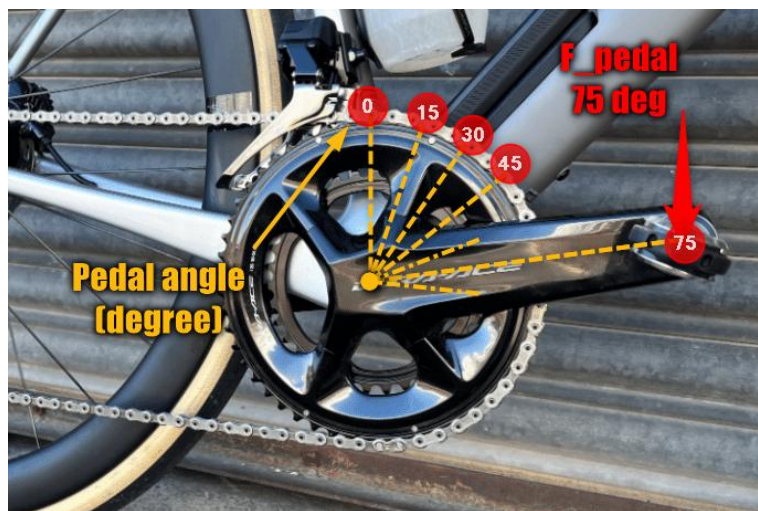


Figure 7. Pedaling cycle segmentation (every 15 degrees)

Finally, the chosen dataset corresponds to a standard scenario of eBike use, so that the test matches as closely as possible the most frequent conditions of use for the DU: no uphill/downhill slope, electric assistance running, middleweight cyclist.

3.2 Pedaling cycle simulation

3.2.1 DU model and configuration

3.2.1.1 Model simplifications

As mentioned earlier, the finite element DU model was taken from a previous student and was already simplified compared to the real model. However, for the needs of the study, some other modifications were also applied. Indeed, the rotor, stator, all the different shafts and gearings inside the BDU have been removed and only the motor casings (housing on the left side and cover on the right side), the bearing bracket and the outer ring of the bearings connecting the shafts to the cover/housing have been retained. Since all the constraints of the DU are known, it is possible to reproduce these constraints with only this configuration: the essential part of the motor connected to the bike frame. The aim was to keep only the relevant part for the finite element simulation. Thanks to that simulation models are simplified and require fewer computational resources. Figure 8 is representing a cross-section of the model used for the study.

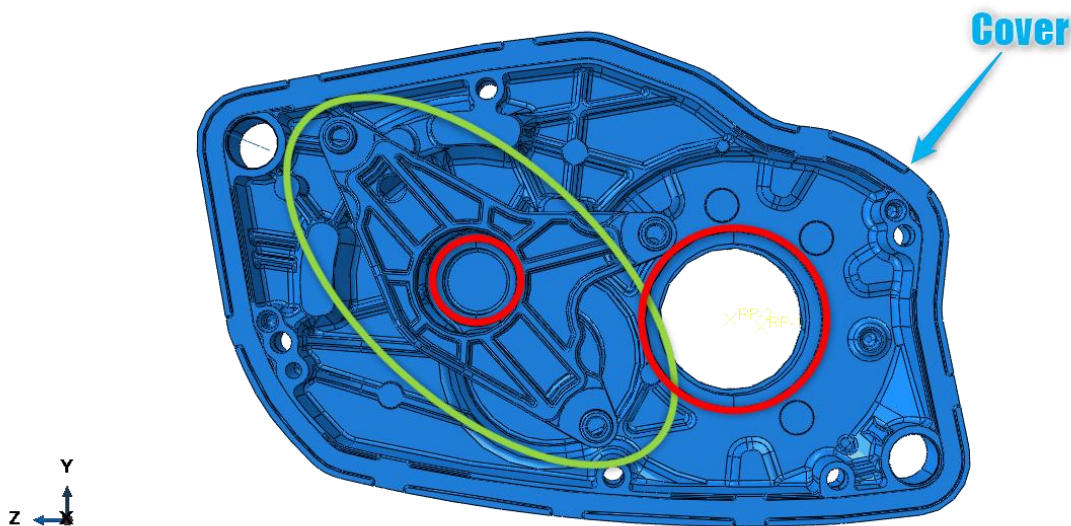


Figure 8. YZ DU cross-section highlighting the bearing bracket (green) and some bearing outer rings (red)

Inside the DU, there was originally three different shafts: the rotor shaft, the intermediate shaft and the crankshaft (linked to the pedals). They are all connected to the housing/cover with 6 bearings, 2 bearings for each shaft, mounted inside the cover, the housing or the bearing bracket. Shafts transmit stress to the rest of the DU through these bearings. All these shafts have been removed, but their effect and the stresses on the DU they are responsible for will still be considered thanks to the outer bearing rings that were introduced in the model. In fact, all the efforts they apply to the DU are focused on the bearings.

These outer bearing rings are connected to the other pieces of the model thanks to a tie constraint. This is a feature used to connect two surfaces such that they behave as a single, inseparable unit, there is no slip, separation, or penetration allowed between the tied surfaces and the forces/moments are transferred directly across the interface. Moreover, the pedal forces will also be applied on those bearings, indeed all the forces applying on the DU will be replaced by their equivalent forces on the 6 corresponding outer bearing rings. The equivalent loads calculus and establishment will be detailed in the next section ([1.2.2 Equivalent bearing forces](#)).

3.2.1.2 Boundary conditions

The constraints in the DU arise from the fact that forces are applied to the electric motor, but that it is fixed to the bicycle frame and therefore constrained by it. Here, the attachment to the frame has been reproduced on the FEM model. Fastening screws have been added to the model in the designated locations to reproduce as accurately as possible the DU fixation. The location of these screws can be seen in Figure 9:

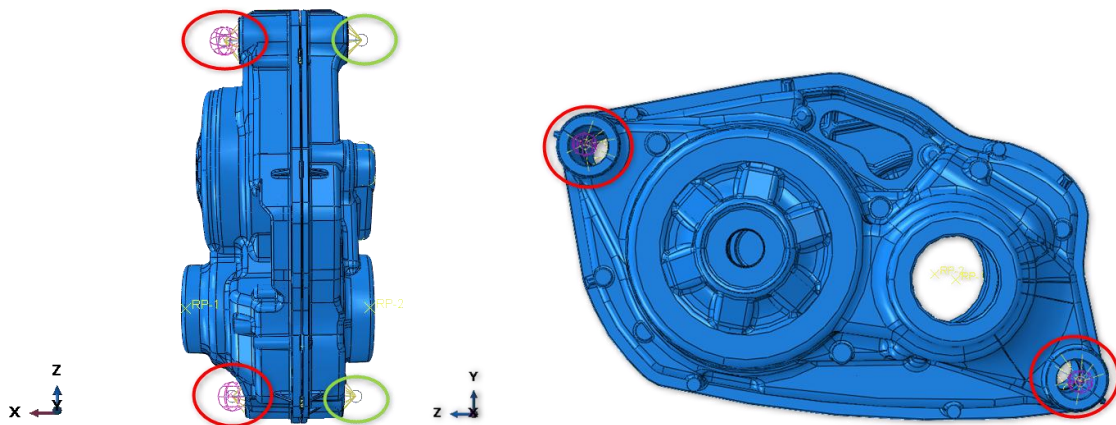


Figure 9. Fastening screws (left ones in red and right ones in green)

Both right screws do not allow any degree of freedom, they have an encastre function (they are flush-mounted). However, both left screws allow two degrees of freedom (translation according to Y and Z axis), they play here the role of springs/dashpots, blocking all other degrees of freedom and providing a certain stiffness according to Y and Z axis.

3.2.2 Equivalent bearing forces

3.2.2.1 Model Loads

The last elements needed for the simulation are the model loads. The 3D pedaling forces from the data cannot be directly applied on the current simulation model as a lot of pieces from it have been removed. This is why, as mentioned in the last section, the aim is to use the equivalent forces acting on the bearings. The aim is to calculate for each

step (static Abaqus simulation for each point of the pedaling cycle), the equivalent bearing forces thanks to mechanical equilibrium calculus, based on the data acquisition (3D pedaling forces, motor moment and pedal angle). From these equivalent bearing forces, it will be possible to apply the corresponding loads on the bearing outer rings of the simulation model.

As the mechanical equilibrium calculus is complex, the task will be divided into two subtasks. Different forces are acting on the DU, there are inside and outside forces. The shafts equilibrium, regarding inside BDU forces, will be calculate first then the crankshaft equilibrium considering all forces in a second step:

- Calculation of the equilibrium of the shafts and gearing inside the DU: considering only the motor torque, the corresponding forces/moment and no pedaling forces. It will give access to the bearing forces of the rotor and intermediate shafts, and to gearing force induced by the motor acting on the crankshaft.
- Calculation of the crankshaft equilibrium: considering the forces/moments outside the DU (pedal forces, chain force) and the motor induced gearing force/moment, calculated previously.

For a better understanding of the problem, the forces acting on the different shafts of the DU are presented in Figure 10:

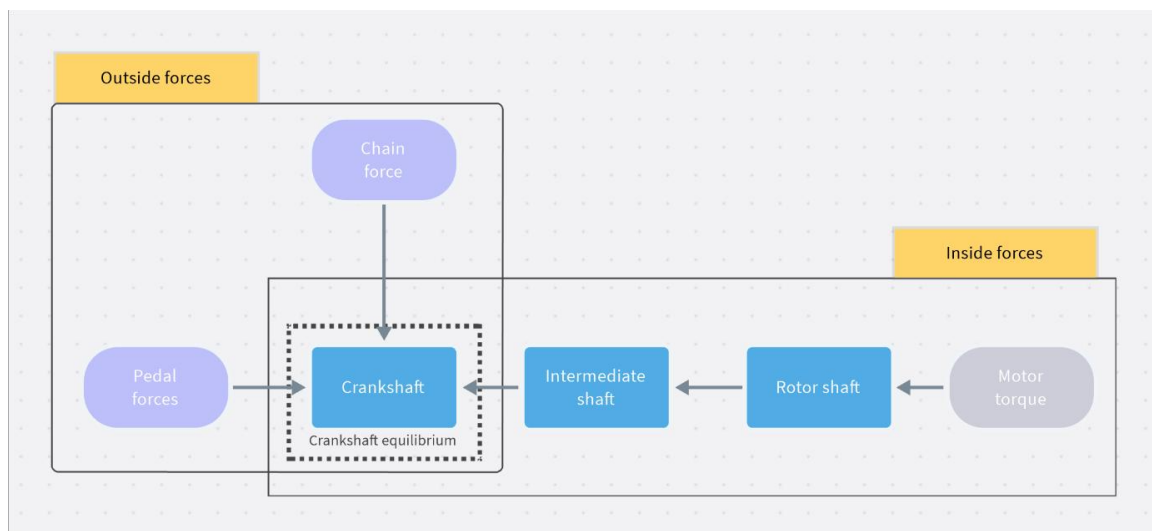


Figure 10. DU force flow chart

Once the equilibrium is calculated, all the information needed for the equivalent bearing forces are accessible and loads can be applied.

3.2.2.2 Motor induced mechanical force component: Shafts and gearing equilibrium

This section is devoted to calculating the force equilibrium of the shafts and gears inside the BDU to define the stress induced by the electric assistance on the DU when it is operating. This will partly give access to the bearing reaction forces inside the DU while

the electric motor is running. For this part, the effect of forces applied outside the DU (pedal forces and chain force) will not be considered. It will therefore also be necessary to take into account the effects of these other forces later on.

To calculate the shafts and gearing mechanical equilibrium, the starting point is the torque induced by the electric motor. Inside the DU, three shafts are in contact: the rotor/motor shaft (shaft number 1) transmits movement and force to the intermediate shaft (shaft number 2) via a gear, and the same phenomenon occurs between the intermediate shaft and the crankshaft (shaft number 3). This is how electric assistance is created for the bicycle user. However, these interactions induce forces on these shafts, and they need to be calculated for the needs of the simulation. Figure 11 provides an overview of the shafts and gearing system:

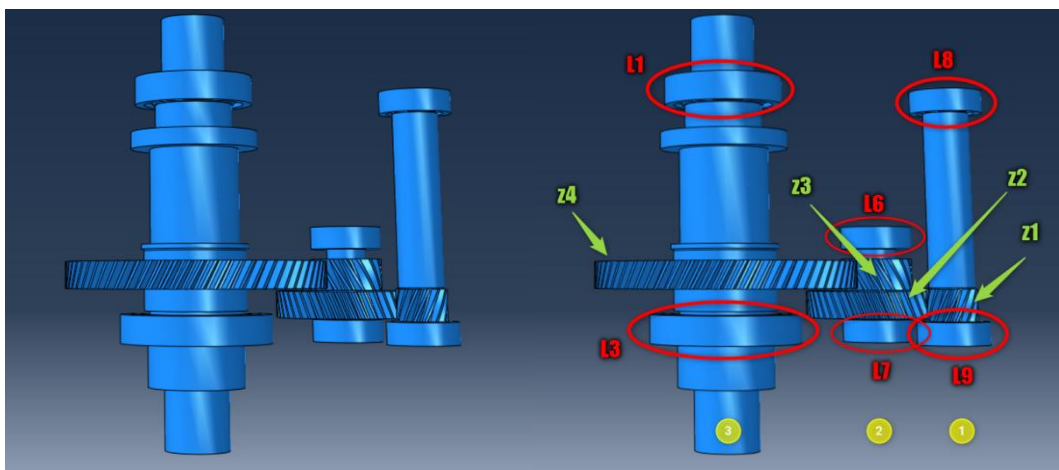


Figure 11. Shafts and gearing configuration inside the DU (shafts in yellow, gearing in green and bearings in red)

Usually, the DU simulation team request these calculations from the BOSCH research department, which are performed using mechanical simulation software called KISSsys. However, this approach has several drawbacks: the DU simulation team is not independent because it needs assistance from another department to perform its tasks. Furthermore, having to ask for help and not possessing the necessary expertise directly slows down the task, not to mention that increasing the number of intermediaries can add errors to the process (communication errors, human error, etc.). Once again, the goal of this study is to be able to deploy a turnkey simulation solution for the DU simulation team, so it was decided with the thesis supervisors that the calculation of the forces induced by the electric assistance would be performed using a spreadsheet or a Python script.

3.2.2.2.1 Mechanical system and equations

So, the goal will be to consider the set of three shafts as a static system and calculate its equilibrium (forces induced inside the system and the bearing reaction forces of each shaft) under a certain motor torque, using the previous KISSsys calculations as a reference to verify the results of the calculations performed. The simplified shaft system

is detailed in Figure 12. Simplifications will be made; shaft deformation and dynamic effects will not be considered; only static equilibrium equations will be considered. Moreover, the electric motor cannot have a negative torque and if it is not running, zero torque means no stress on the shafts and therefore no bearing reaction force.

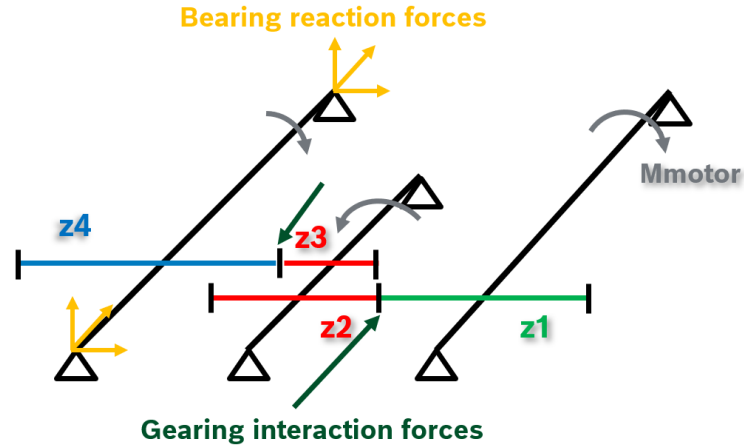


Figure 12. Shafts and gearing simplified system

Once all this has been established, the next step is to establish the equilibrium equations for the system. There is first the force equilibrium, with equations (1), (2) and (3), which concerns each shaft 1, 2 and 3 (forces are in N):

$$X_L + X_R = \sum_{i \in \{1,2,3,4\}} FX_{-z_i} \quad (X \text{ axis}) \quad (1)$$

$$Y_L + Y_R = \sum_{i \in \{1,2,3,4\}} FY_{-z_i} \quad (Y \text{ axis}) \quad (2)$$

$$Z_L + Z_R = \sum_{i \in \{1,2,3,4\}} FZ_{-z_i} \quad (Z \text{ axis}) \quad (3)$$

with:

- X_L & X_R : the X-axis force component of the reaction forces of the left bearing (L1, L6 or L8) and right bearing (L3, L7 or L9) on the shaft
- Y_L & Y_R : the Y-axis force component of the reaction forces of the left bearing (L1, L6 or L8) and right bearing (L3, L7 or L9) on the shaft
- Z_L & Z_R : the Z-axis force component of the reaction forces of the left bearing (L1, L6 or L8) and right bearing (L3, L7 or L9) on the shaft
- $\sum_{i \in \{1,2,3,4\}} FX_{-z_i}$: the sum of X-axis force components of the gear interaction forces applied on the shaft
- $\sum_{i \in \{1,2,3,4\}} FY_{-z_i}$: the sum of Y-axis force components of the gear interaction forces applied on the shaft

- $\sum_{i \in \{1,2,3,4\}} FZ_{z_i}$: : the sum of Z-axis force components of the gear interaction forces applied on the shaft

The gear interaction force nomenclature indicates the name of the gear applying the force. For example, F_{z_1} is the force applied by gear z1 on the resistant shaft with which it is in contact, i.e., shaft 2. Consequently, the only gear interaction force acting on shaft 1 is F_{z_2} , the only one acting on shaft 3 is F_{z_3} , and shaft 2 experiences the effect of the gear interaction forces F_{z_1} and F_{z_4} .

Then, the moment equilibrium for each shaft is established in equations (4) and (5) (moments are in Nm and the moment equilibrium is calculated at the point equidistant from the two bearings):

$$MY_{Z_L} + MY_{Z_R} = \sum_{i \in \{1,2,3,4\}} MY_{FZ_{z_i}} + \sum_{i \in \{1,2,3,4\}} MY_{FX_{z_i}} \quad (Y \text{ axis}) \quad (4)$$

$$MZ_{Y_L} + MZ_{Y_R} = \sum_{i \in \{1,2,3,4\}} MZ_{FY_{z_i}} + \sum_{i \in \{1,2,3,4\}} MZ_{FX_{z_i}} \quad (Z \text{ axis}) \quad (5)$$

with:

- MY_{Z_L} & MY_{Z_R} : the Y-axis moment induced by Z-axis component of the reaction forces of the left bearing and right bearing on the shaft
- MZ_{Y_L} & MZ_{Y_R} : the Z-axis moment induced by Y-axis component of the reaction forces of the left bearing and right bearing on the shaft
- $\sum_{i \in \{1,2,3,4\}} MY_{FX_{z_i}}$: the sum of Y-axis moment induced by X-axis force components of the gear interaction forces applied on the shaft
- $\sum_{i \in \{1,2,3,4\}} MZ_{FX_{z_i}}$: the sum of Z-axis moment induced by X-axis force components of the gear interaction forces applied on the shaft
- $\sum_{i \in \{1,2,3,4\}} MZ_{FY_{z_i}}$: the sum of Z-axis moment induced by Y-axis force components of the gear interaction forces applied on the shaft
- $\sum_{i \in \{1,2,3,4\}} MY_{FZ_{z_i}}$: the sum of Y-axis moment induced by Z-axis force components of the gear interaction forces applied on the shaft

There is no equation for the moment following X because the shafts rotate around it. Moments from the X-component gear reaction forces are nevertheless integrated into the equations for the moment following the Y and Z axes, as highlighted in Figure 13:

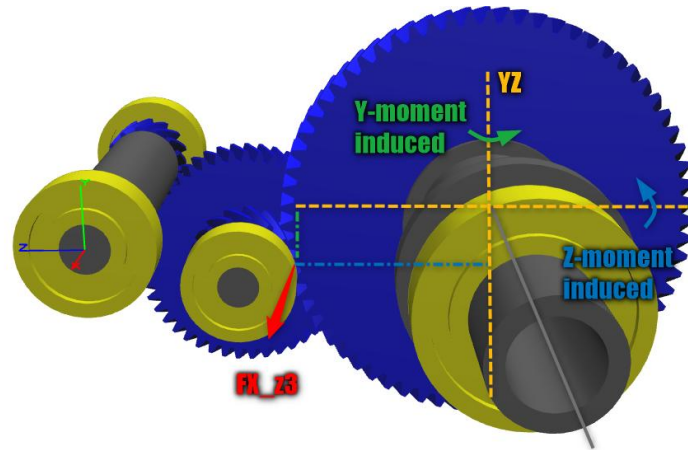


Figure 13. Moments induced by X-component of gear interaction force

3.2.2.2.2 Gearing interaction forces

The interaction forces ($F_{z_1}, F_{z_2}, F_{z_3}, F_{z_4}$) between the helical gears were calculated using the following scientific work: “Gear geometry and applied theory” (p400-401) [9]. The components of the contact force between two gears (driving gear and driven gear), applying on the contact point P, are detailed in Figure 14 and derived in Figure 15 [9]:

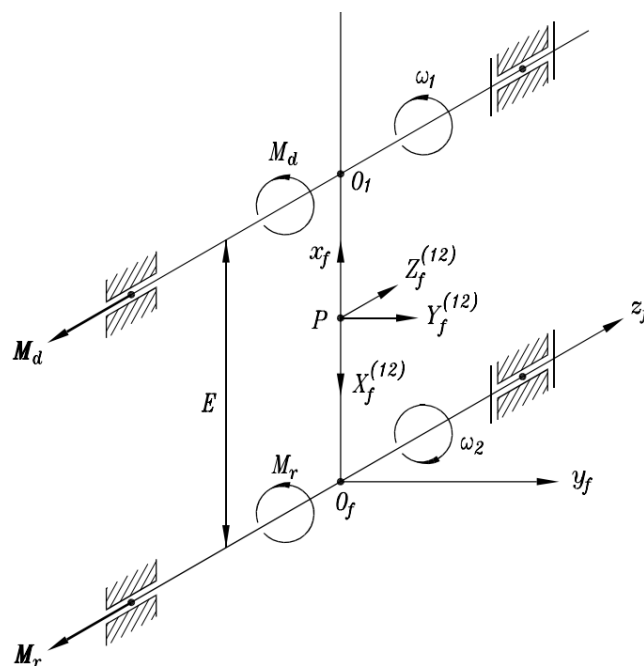


Figure 14. Components of helical gears contact force

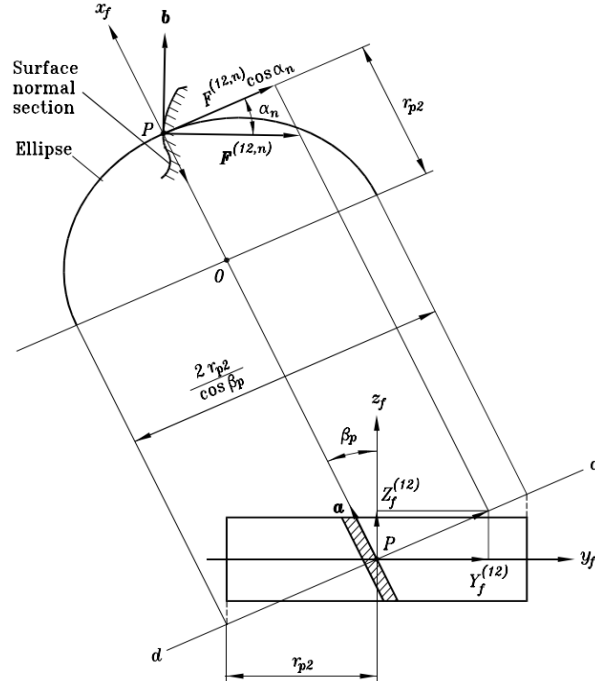


Figure 15. Derivation of components of contact force

The driving gear (gear above) has a moment M_d and make the second gear (below) turn and apply on it a contact force whose components are in the (x_f, y_f, z_f) coordinate system (friction is neglected) [9]:

$$\text{Radial force : } X_f = -\frac{M_r}{r_{p2}} \times \frac{\tan \alpha_n}{\cos \beta_p} \quad (6)$$

$$\text{Tangential force : } Y_f = \frac{M_r}{r_{p2}} \times \tan \beta_p \quad (7)$$

$$\text{Axial force : } Z_f = \frac{M_r}{r_{p2}} \quad (8)$$

With the known data of the DU gearings:

- M_r : resisting moment of driven gear
- α_n : rack profile angle in normal section
- β_p : helix angle
- r_{p2} : radius of the driven gear

And the total force on the driven gear is:

$$F_{tot} = \frac{M_r}{r_{p2} \cdot \cos \alpha_n \cdot \cos \beta_p} \quad (9)$$

Thanks to these results, all the components (radial, tangential, axial) of the gearing contact forces can be calculated from the electric motor torque and geometric parameters of the DU, in the coordinate system (x_f, y_f, z_f) . All that remains is to project these components in the global coordinate system of the Abaqus DU simulation model (x, y, z) , to obtain the specific terms of the equations:

- $\vec{F}_{-z_1} = [FX_{-z_1}, FY_{-z_1}, FZ_{-z_1}]$
- $\vec{F}_{-z_2} = [FX_{-z_2}, FY_{-z_2}, FZ_{-z_2}]$
- $\vec{F}_{-z_3} = [FX_{-z_3}, FY_{-z_3}, FZ_{-z_3}]$
- $\vec{F}_{-z_4} = [FX_{-z_4}, FY_{-z_4}, FZ_{-z_4}]$

and consequently: $\sum_{i \in \{1,2,3,4\}} FX_{-z_i}$, $\sum_{i \in \{1,2,3,4\}} FY_{-z_i}$, $\sum_{i \in \{1,2,3,4\}} FZ_{-z_i}$.

Moreover, the mechanical properties of the DU imply for each shaft that, one of the bearings has an X-axis reaction force component which is null:

$$X_{L3} = X_{L7} = X_{L9} = 0 \text{ N} \quad (10)$$

This means that, for each shaft, there is a system of 5 mechanical equations (3 force equilibrium equations and 2 moment equilibrium equations) and 5 unknowns which are the components of the bearing reaction forces of the shaft: either X_L or X_R , Y_L , X_R , Z_L and Z_R . These systems can now be solved.

Finally, the results obtained are relatively accurate: the calculated bearing reaction forces have an error of less than 10% compared to the results from the KISSsys software. This is satisfactory regarding all the simplifications made. The calculations for these tasks are therefore fully automated and adaptable to any other BOSCH eBike electric motor, as they are entered into an Excel spreadsheet. This will serve as the basis for the Python script used to automate the entire simulation process of the study.

The results obtained will then make it possible to determine the exact forces and moments acting on the crankshaft in the presence of motor assistance. Added to this are the stresses caused by forces outside the DU (3D pedal forces and chain force). Both combined enable to determine all the stresses to which the DU is subjected using once again the equations of static mechanical equilibrium: including this time all the forces acting on the crankshaft.

3.2.2.3 Global DU mechanical equilibrium

The aim here is to calculate the mechanical equilibrium of the crankshaft, considering all the forces acting on it. The forces acting on the other shafts have already been determined by the calculation performed in the previous section; only the crankshaft equilibrium needs to be recalculated, taking into account the motor-induced force and moment (F_{-z_3} and $M_{F_{-z_3}}$) and the forces from outside the BDU.

As already said, the forces acting on the crankshaft from outside the DU are the 3D pedal forces and the chain forces, an example of the force's configuration is presented in Figure 16:

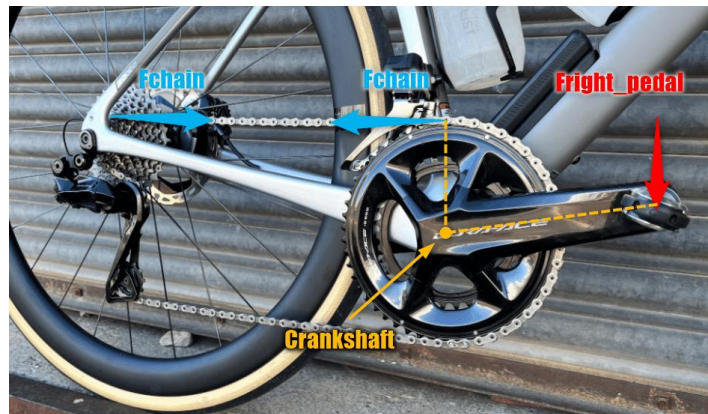


Figure 16. Force configuration on the crankshaft (pedal force on the right side only)

The mechanical system can be simplified as follows in Figure 17 (keeping in mind the moments and forces considered are in 3D):

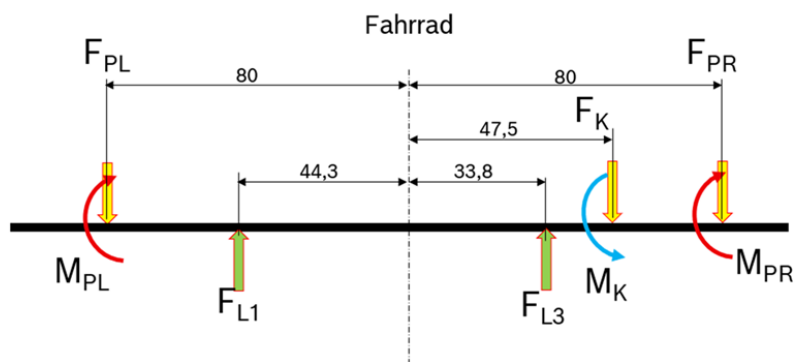


Figure 17. System simplification of the crankshaft

All the measurements are in millimetres mm , the indexes “PL” and “PR” stand for “Pedal Left”, “Pedal Right”, then, “L1” and “L3” represent the left and right bearing on which the crankshaft rests. Finally, “K” stands for “Kette”, the chain in German.

The global crankshaft mechanical equilibrium, including the motor induced component, would be described by the following system shown in Figure 18:

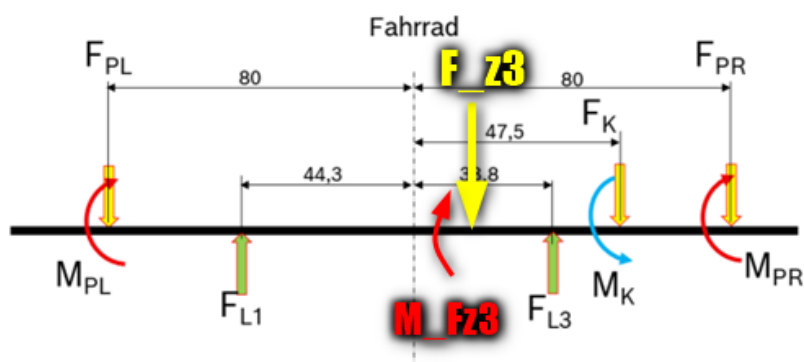


Figure 18. Simplified system including motor induced force and moment

This system is described by the following mechanical equations, from (11) to (15). Left part of the force equations are still the bearing force reactions and left part of the moment equations are still the bearing moment reactions to the forces acting on the shaft (forces in N , moments in Nm and the moment equilibrium is calculated at the point equidistant from the two bearings):

$$X_{L1} + X_{L3} = \sum FX_{Pedal\ forces} + FX_{-z3} \quad (X\ axis) \quad (11)$$

$$Y_{L1} + Y_{L3} = \sum FY_{Pedal\ forces} + FY_{-z3} \quad (Y\ axis) \quad (12)$$

$$Z_{L1} + Z_{L3} = \sum FZ_{Pedal\ forces} + FZ_{-z3} + F_K \quad (Z\ axis) \quad (13)$$

and,

$$MY_{Z_{L1}} + MY_{Z_{L3}} = \sum MY_{FZ_{Pedal\ forces}} + \sum MY_{FX_{Pedal\ forces}} + MY_{FX_{-z3}} + MY_{F_K} \quad (Y\ axis) \quad (14)$$

$$MZ_{Y_{L1}} + MZ_{Y_{L3}} = \sum MZ_{FY_{Pedal\ forces}} + \sum MZ_{FX_{Pedal\ forces}} + MZ_{FX_{-z3}} \quad (Z\ axis) \quad (15)$$

with:

- $\sum FX_{Pedal\ forces}$, $\sum FY_{Pedal\ forces}$, $\sum FZ_{Pedal\ forces}$: the sum of the X, Y and Z components of the 3D pedal forces
- F_K and MY_{F_K} : such as the chain force $\vec{F}_K = [0, 0, F_K]$ induces an Y-axis moment MY_{F_K}
- (X_{L1}, Y_{L1}, Z_{L1}) and (X_{L3}, Y_{L3}, Z_{L3}) : the different components of the bearing L1 and L3 reaction forces
- $MY_{Z_{L1}}$ and $MY_{Z_{L3}}$: Y-axis moments induced by the Z-axis component of the bearing reactions forces of L1 and L3
- $MZ_{Y_{L1}}$ and $MZ_{Y_{L3}}$: Z-axis moments induced by the Y-axis component of the bearing reactions forces of L1 and L3
- $\sum MY_{FX_{Pedal\ forces}}$ and $\sum MZ_{FX_{Pedal\ forces}}$: the sum of the Y-axis moments and the Z-axis moments induced by X-axis component of the pedal forces
- $\sum MY_{FZ_{Pedal\ forces}}$: the sum of the Y-axis moments induced by Z-axis components of the pedal forces
- $\sum MZ_{FY_{Pedal\ forces}}$: the sum of the Z-axis moments induced by Y-axis components of the pedal forces

On this shaft, the DU mechanical properties imply that $X_{L3} = 0\ N$, so the unknown of the problem are only $X_{L1}, Y_{L1}, Y_{L3}, Z_{L1}$ and Z_{L3} . There are 5 equations for 5 unknowns, so

the system can be solved. Once these equations and the one from the previous section are solved, all the bearing reaction force values are accessible, and therefore, the loads applying on the bearings (outer bearing ring), which are the inputs needed for the FEM simulation, are also known. Indeed, the forces applying on the bearings are the opposite of the bearing reaction forces and as the measurements of the bearings are known, the loads applying on the bearings are also known (applying: pressure = force/surface).

Thus, for each point/each angle of the pedalling cycle, it will be possible to calculate the loads applying on the bearings of the DU, to provide them to Abaqus to launch the FEM simulation. However, this action will require an additional step to be performed correctly, which will be explained in the following section.

3.2.2.4 DLOAD subroutine

To apply the correct bearing loads, calculated from the mechanical equations, on the DU simulation model, the use of an additional DLOAD subroutine will be required. The DLOAD subroutine in Abaqus is a powerful tool for simulating complex loads that vary with spatial coordinates, element number or time. This tool takes the shape of a FORTRAN language script, which will be called at each load integration point for each element-based or surface-based nonuniform distributed load definition during stress analysis in Abaqus. It allows users to apply user-defined distributed loads, such as pressure or body forces, that can change based on previously mentioned factors.

The subroutine is required for the FEM simulation, because it allows for more accurate results, closer to reality. In fact, the standard method of applying a load in Abaqus only allows a uniform load to be applied, which does not correspond to the mechanical configuration of the shafts and bearing contact zone.

The configuration of the shafts and the bearings corresponds to a cylinder-cylinder contact case; there is a contact between a male cylinder and a female cylinder, see Figure 19:

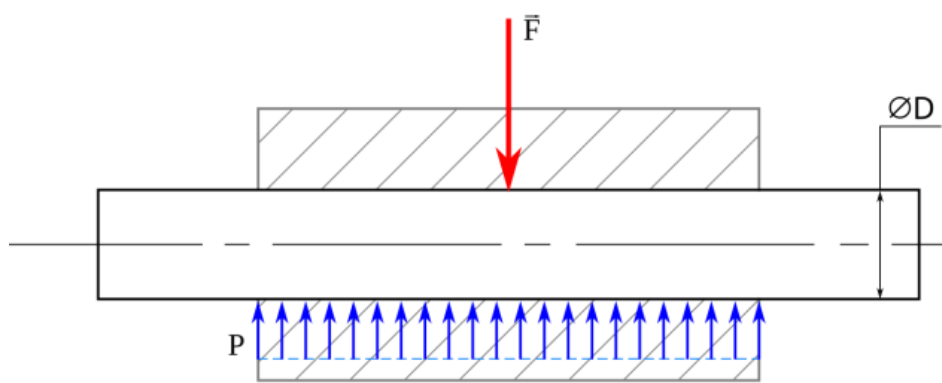


Figure 19. Contact configuration between the shaft (white) and the bearing (striped)

There are different ways to describe the pressure repartition on the contact zone between the shaft and the bearing, according three different cases: the parts are rigid

bodies (a), the parts are elastic bodies but the clearance is neglected (b), and the parts are elastic bodies and the clearance is not ignored (c). They are summarized in Figure 20 [10]:

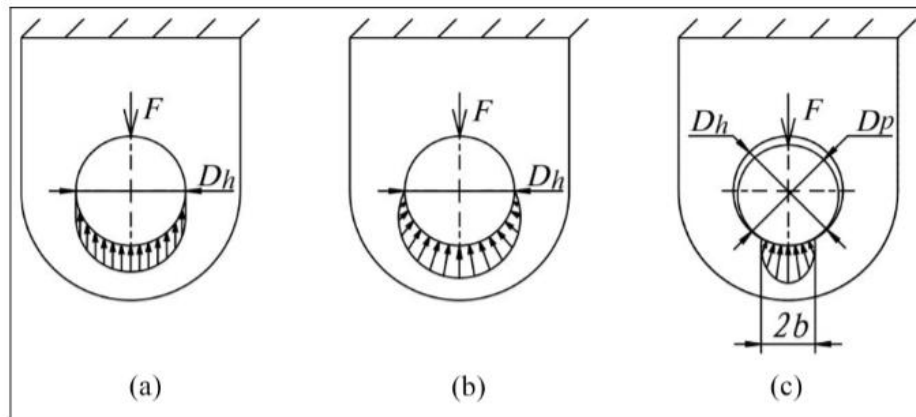


Figure 20. Shaft/bearing contact pressure distribution model ((a) uniform pressure distribution model, (b) sinusoidal pressure distribution model, and (c) Hertz pressure distribution model)

In the case of this DU, the parts are elastic bodies, and the clearance can be neglected, because the system shaft/bearing is not in the range of application of the Hertz theory (case c, Hertz theory requires $\frac{D_h}{D_p} > 1,02$) [10]. Therefore, pressure distribution model is not uniform (case a., corresponds to the Abaqus load repartition), but it is a sinusoidal pressure repartition (case b.), which is described in Figure 21 [11], [12]:

$$P_{\max} = \frac{4}{\pi} \cdot \frac{F}{LD}$$

$$P(\theta) = P_{\max} \cdot \cos \theta$$

Figure 21. Sinusoidal pressure distribution model description

This load case cannot be applied directly through Abaqus (which uses case (a)), this is why a FORTRAN DLOAD subroutine is needed. The DLOAD subroutine only applies a user-defined pressure in 2D, and the UTRACLOAD subroutine establishes the traction stress/axial stress between the shaft and the bearing. Both subroutines are in the same FORTRAN script, and they work the same way. When configuring the Abaqus simulation model, at the surfaces where you want to apply the pressure profile and traction load, you indicate to Abaqus that they are user defined. Thus, during the simulation, Abaqus reads the FORTRAN script and knows which pressure profile is associated with which surface. A simplified diagram of the ABAQUS subroutine process illustrating this is shown in Figure 22:

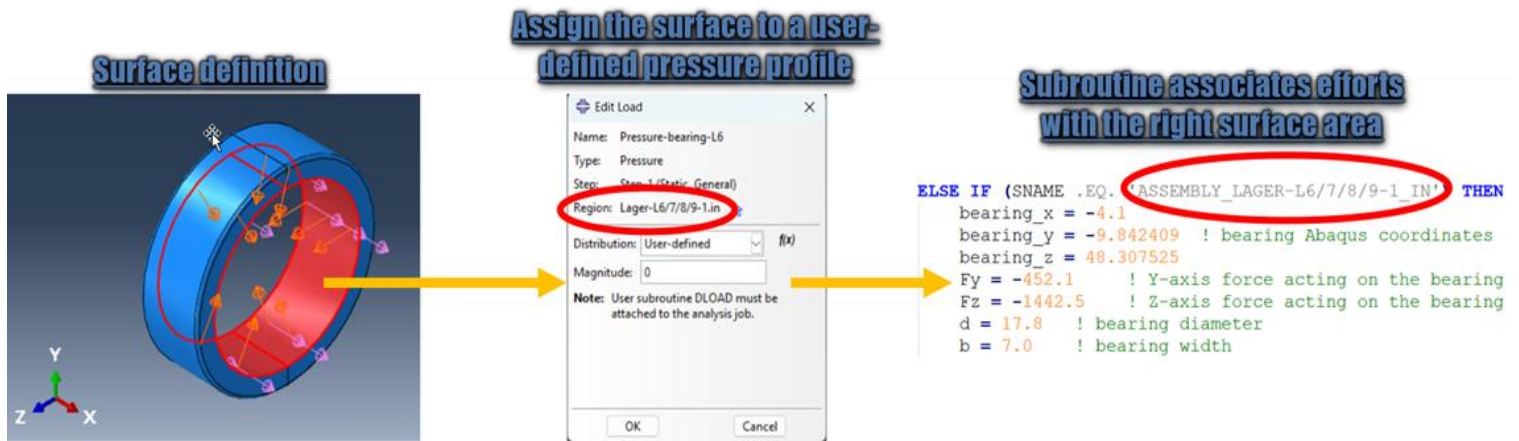


Figure 22. Abaqus subroutine process

A simplified example of subroutine script used for the study is available in the appendix ([Appendix 3 and 4: Figures A-3 and A-4](#)). Finally, to launch the FEM simulation in Abaqus with user-defined distributed loads, the FORTRAN corresponding script must be joined manually to the input file, for the simulation to be realized properly.

3.3 Abaqus processing and workflow automation

After discussing pedaling data, explaining how it would be used in this study, and then deducing the bearing forces, which are the input parameters of the simulation, this section is dedicated to the different file processing within the Abaqus operating mode.

3.3.1 Abaqus operating mode and choice of use

Back on the simulation process, Figure 23 highlights the process of running an ABAQUS simulation:

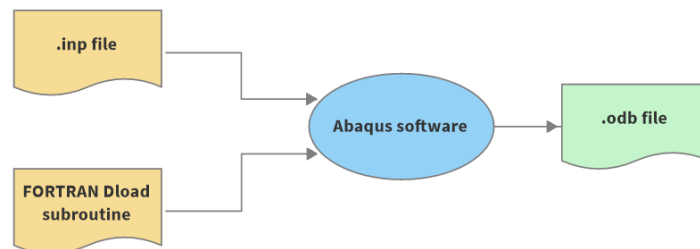


Figure 23. Abaqus simulation procedure (input files in orange and output files in green)

In fact, the input (.inp) is summarizing all the information of the simulation (parameters and geometry of the finite element model, simulation steps, ...), and the FORTRAN file enables to provide the user defined pressure profile: these two files are the input of the simulation for the software Abaqus. After running, Abaqus produces an output file (output data base file) regrouping all the results of the simulation.

The aim of this study is to simulate an entire pedaling cycle containing 24 distinct points every 15 degrees of pedal angle (from 15 to 360 degrees). There are therefore two

possible directions summarized in Figure 24: either perform a simulation comprising the 24 steps previously entered or perform one simulation per 15-degree increments:

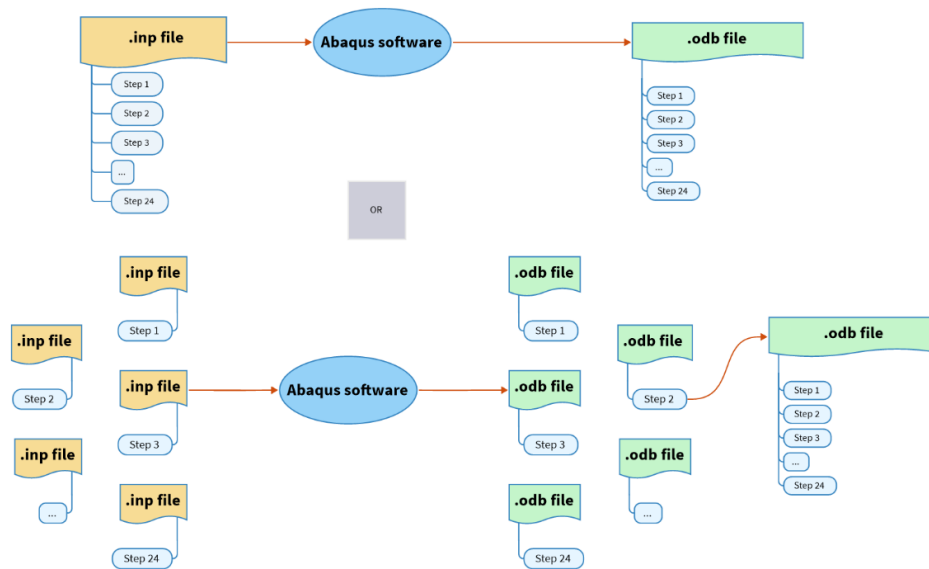


Figure 24. Both simulation scenarios

The most effective and practical way to proceed would have been to perform a unique Abaqus simulation including all the 24 steps. Performing a unique simulation means that every piece of information is gathered in the same input file and Abaqus produces a unique output file summarizing all the results. In the other case Abaqus would have to process 24 different input files and produce 24 separate output files that would have had to be manually recomposed. However, the constraints on the bearings during simulation change at each stage of the simulation (every 15 degrees), which means that one different subroutine is required per 15-degree step, but Abaqus only accepts a single FORTRAN Dload/Utracload subroutine per input file; scenario 2 had been chosen. In addition, in the case of the study, the .inp files for each step are the same, as long as the only things which change, between a step of the simulation and the next one, are the bearing forces and pressure, defined in the Dload/Utracload subroutine file (models parameters defined in the .inp file stayed unchanged). A few minor changes will be made to optimize the calculation time and compilation of .odb files. These will be detailed in the following section.

Finally, the simulation proceeds as follows: the .inp file is provided to Abaqus with the FORTRAN subroutine corresponding to the simulated step. Once the simulation is complete, the operation is repeated for the next step, with the same .inp file, but with the FORTRAN subroutine corresponding to next pedal angle. At the same time, an Abaqus command is called to compile the .odb files into a single original .odb file as they are calculated.

The different stages executing at each step are detailed in Figures 25 and 26:

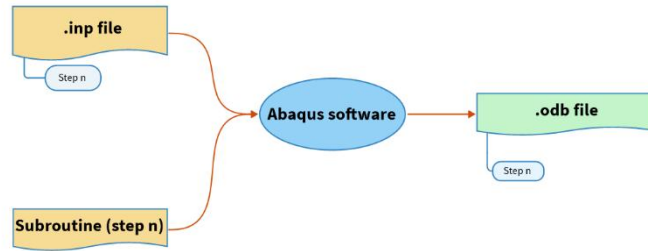


Figure 25. Step n of the simulation - Stage 1: simulation of the step n

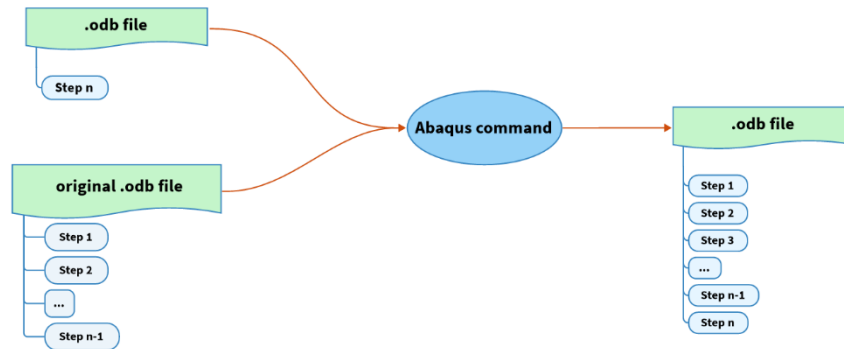


Figure 26. Step n of the simulation - Stage 2: compiling results of step n with all the previous steps

This loop is repeated until the step 24, so that at the end of the simulation the original .odb file contains the results of every 15 degrees interval, from 15 to 360 degrees. Thus, at this point, it is possible to calculate and establish the inputs of the simulation (cf. [3.1.2 Pedaling cycle simulation](#)), and the method of using ABAQUS in the context of this study has just been developed in this section. The final clarifications of this work will be provided on the automation of the working method.

3.3.2 Workflow automation

Indeed, up to this point, several aspects of the entire task have been addressed and detailed. This section therefore aims to gather them and organize them in order to create a structured and effective working method. A significant part of this thesis subject was to automate the workflow with different codes and languages, once the method has been established previously. Automating engineering workflows enables to improve the working efficiency, enhance its quality and thus reduce the costs (labor costs, time-relative costs, etc.). What is interesting is that automation allows other engineers to easily adopt the previously established method and its working tools, and ensures consistent, high-quality outcomes, by eliminating repetitive tasks, minimizing human error, streamlining and gathering processes.

As mentioned above, the automation includes different languages, and each has a specific function:

- Python: for data processing, simulation loads calculation and subroutine creation
- Shell script: inp. files creation, running simulation and combinings .odb files

Their operation will be detailed in the following sections.

3.3.2.1 Python automation

The role of the automation with Python language is to manage the pedaling data in order to create the FORTRAN Dload/Utracload subroutine scripts corresponding to the 24 chosen steps of the simulation. Figure 27 provides a quick overview of how it works:

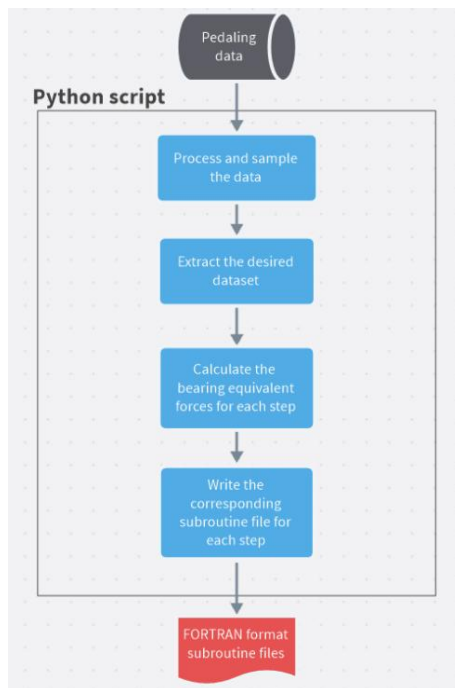


Figure 27. Python automation script operating mode

This python script is divided into three parts:

- Pedaling data part: This part aims to treat and sample the data in order to create Python easy to use data frames. The nature of the dataset can be chosen (regular road, uphill data, etc.) , and the sampling rate can be adjusted (in how many steps the pedaling cycle is divided).
- Bearing equivalent forces calculation function: From the selected dataset and specified geometric parameters of the BDU, this function aims to calculate the equivalent bearings forces applying on the simulation model. The function returns a Python Dataframe (two-dimensional, tabular data structure) containing the X, Y and Z components of the equivalent bearing forces applying on each bearing (L1, L3, L6, L7, L8, L9). It can be adapted and works for any other BDU model; simply enter the geometric parameters of the new BDU model.

- **Subroutines creation function:** This function is creating the necessary FORTRAN subroutines for each step of the simulation from the equivalent bearing forces Dataframe calculated and the bearings geometric parameters of the DU.

Finally, the python script produces all the necessary matter to run the Abaqus simulation step by step. And this last step is performed by simply launching a shell script in a terminal.

3.3.2.2 Shell script automation

To automate the simulation of the 24 steps, it is necessary to create a shell script that will automatically launch these simulations. Abaqus does not allow to do this; the 24 simulations should have been launched manually.

After configuring the BDU simulation model, it is possible to generate the original input file (.inp file) necessary for the simulation. The subroutines corresponding to each step of the simulation will have been created beforehand using the Python script. Thus, the shell script is used to launch and automate the Abaqus simulation of each step of the pedaling cycle. The shell script operating mode is detailed in Figure 28:

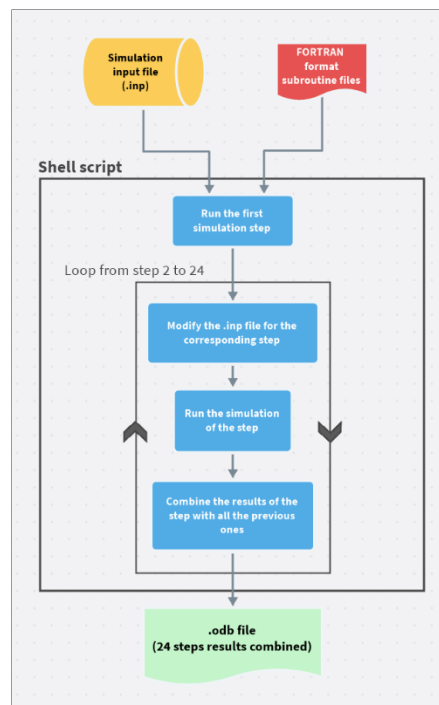


Figure 28. Shell script automation operating mode

This script is also divided into three parts:

- **The .inp file creating function:** Based on the original input file of the first simulation step, this function is creating the input files for the next steps. Actually, the original input file can be used for every steps, however it means that Abaqus is re-reading and re-establishing the model data in the Abaqus environment at every step. Therefore, for reasons of simulation time

optimization and flexibility, the function is creating lighter input files for every step not containing the model data (which will be kept in RAM in Abaqus).

- Simulation of the first step: This simulation is separated from the other steps because the upcoming loop (simulation loop) is calling results from the previous simulation; first step cannot be integrated to the loop.
- Simulation and combination loop: This loop is launching the Abaqus simulation for each step, calling the .inp file creating function and asking Abaqus to resume writing its results from the previous step (which means this avoids having to re-enter the model data in the .inp file at each step, cf. function above). Finally, the loop recombine the results of each step with all the previous ones.

The resulting .odb file can then be opened in Abaqus to view the simulation results. Moreover, the methodology employed for this study has been meticulously documented, providing a comprehensive overview of the approach taken, therefore, the results of the study will be analyzed just after a quick summary of the work routine.

3.4 General summary of the working routine

Since numerous files and software programs are used with this methodology, their roles and interactions are summarized simply in Figure 29:

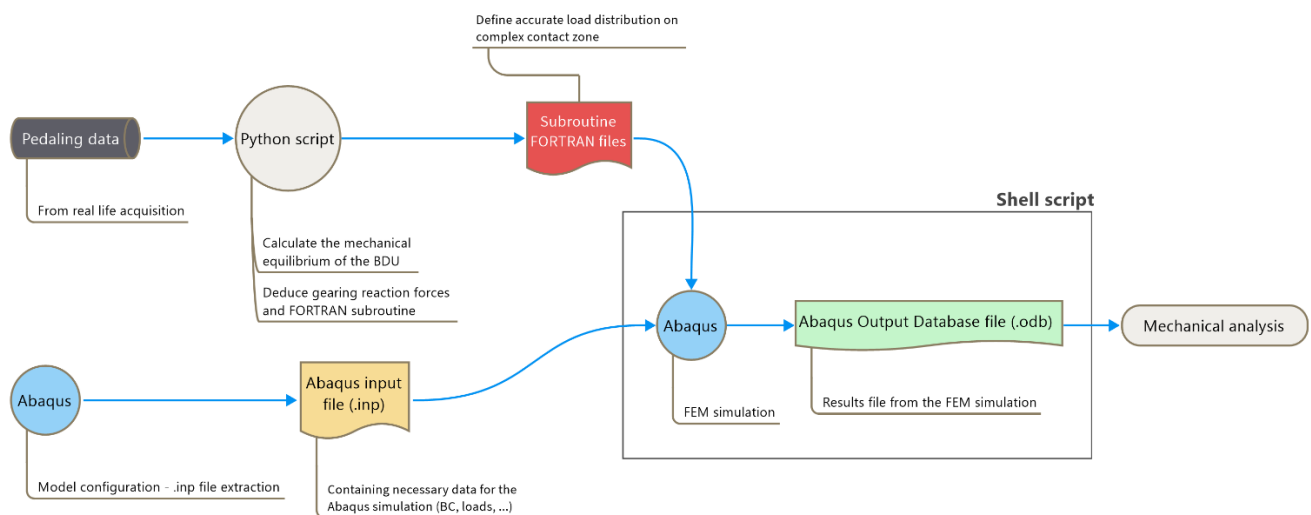


Figure 29. Workflow summary: files and software interactions

Once this summary has been established, it is possible to move on to the mechanical analysis stage. This will present the stresses applied to the DU by a real, normal pedaling cycle. It will then be interesting to analyse the stresses caused by the electric assistance in these results and then finish with a comparison with the ISO standard tests already used.

4. Results

This last part will emphasize the effects of considering triaxial pedaling stress states while the electric motor is running, based on the method previously detailed. The aim will be to investigate whether this enlarged scope of study would be relevant, first by analysing the results of a simple simulation of a standard pedaling cycle. Then, by evaluating the influence of electrical assistance on DU stresses, and finally, by discussing a comparison of this test with ISO norm tests already used by the BOSCH eBike DU simulation team. A part of this section will also be devoted to documenting the study and the transfer of knowledge to the simulation team: how the results and, above all, the study workflow will be transferred to BOSCH.

4.1 Standard pedaling cycle analysis

4.1.1 Chosen dataset

As mentioned previously, this section will present the results of an entire pedaling cycle simulation. This pedaling cycle is not a critical pedaling cycle, this is a standard cycle with electric assistance activated: the cyclist is pedaling at a normal pace, applying basic efforts and the road is neither particularly uphill nor downhill. The chosen input pedaling data can be seen in Figure 30:

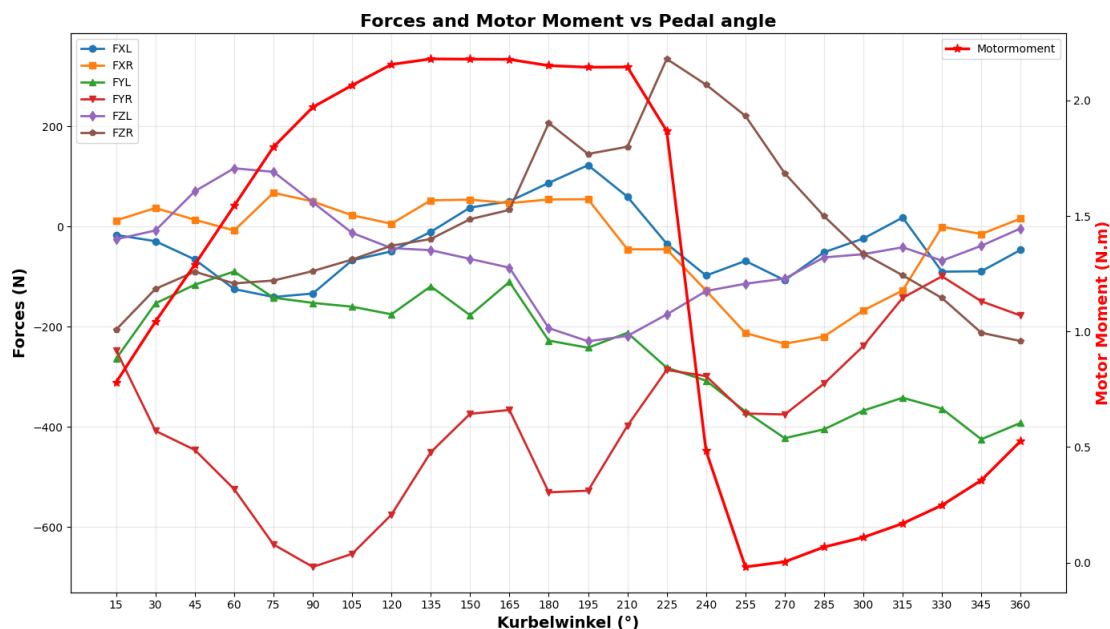


Figure 30. Dataset used for the standard pedaling cycle

This graph represents on the one hand, the X, Y and Z component of the pedaling forces for the left (L) and right (R) pedals, as a function of the pedal angle (Kurbelwinkel). And on the other hand, the electric motor (Motor moment) torque as a function of the pedal angle.

The motor torque varies depending on the pedal angle but remains generally active (50% of the maximum torque at the maximum). Moreover, the maximum force on the pedaling cycle is the right-pedal Y component force, which is around $-700N$, at the angle of 90 degrees. As a reminder, the right pedal in the vertical up position corresponds to the original angle of 0 degrees. Thus, the maximum applied force for both pedals is achieved at the same angle of the pedaling cycle, since the left-pedal Y component force reaches its maximum at the angle of 270 degrees (ca. $-400N$), and the pedals are offset by an angle of π radians. The approximately sinusoidal nature of the Y-axis components of the pedal forces with a phase delay of π radians is also noticeable: this is consistent regarding the pedal offset. However, the component of the right pedal is generally greater. This sinusoidal character with a phase delay can also be observed for the X and Z components of the forces, but these have much lower norms.

4.1.2 Results analysis criterion

This study will analyse the stress states within the eBike electric motor using the von Mises equivalent stress criterion. The von Mises stress is a critical metric in continuum mechanics for predicting the yielding of ductile materials under complex loading conditions. By converting the multiaxial stress state into a scalar value, it provides a practical and simple measure of the overall stress intensity at a point [13]. This approach is particularly relevant for the eBike motor which is composed of a ductile material (metal). In addition, the von Mises criterion allows for a comprehensive assessment of the material's susceptibility to plastic deformation, enabling the identification of potential failure points and the optimization of component design for enhanced durability and reliability.

4.1.3 Simulation results

In order to analyze the results correctly, it is necessary to first discuss the phenomenon of "stress singularities," which are very common when using FEM. These singularities influence the actual results of the simulation, so it is important to know how to recognize them to avoid their effects on the simulation and on the interpretation of the results.

4.1.3.1 Stress singularities

Stress singularities is a complex subject, this study will therefore not go into detail, but it will briefly explore what stress singularities are, why they appear during FEM simulations and why it is important to recognize and avoid them.

In Finite Element Analysis (FEA), the discrete nature of the model and the idealization of boundary conditions often lead to stress concentrations, or "singularities," that are typically absent in physical reality. This phenomenon arises because FEM discretizes a

continuous structure into finite elements, applying forces or constraints at mathematically infinitesimal points, lines, or surfaces. For example, applying a load on a point or imposing a perfect fixed boundary at a sharp corner in a simulation, will produce a theoretical infinite stiffness or infinitely concentrated force causing theoretically a stress approaching infinity [14]. But real-world loads are always distributed over a finite area, and physical fixations possess a degree of compliance, allowing for local stress redistribution. Furthermore, elastic materials can stretch and experience plastic deformation, effectively reducing high stress concentrations and redistributing loads, a phenomenon frequently not taken into account by linear elastic FEM models (a linear model is used for this study). The Saint-Venant's principle largely explains why these localized stress peaks predicted by finite element analysis are often ignored, as their influence decreases rapidly with distance from the point of application [15]. As a result, these high stresses localized near boundary conditions must critically be interpreted, it often requires refining the BC models (e.g., distributed loads, elastic supports) or account for nonlinear models or material behaviors, in order to obtain a more representative picture of the actual stress state of the structure [16].

This study is using a linear simulation model for reasons of reducing the necessary computing power and simulation time. The simulation model is therefore subject to these stress singularities. For example, based on the simulation results, for the 135-degree step, the maximum stress is located near the attachment areas between the bearing bracket and the housing: at the location of a boundary condition. As shown in Figure 31, it can be observed that the maximum stress reaches approximately 130 MPa, and that in general, around other areas where boundary conditions have been created, the stresses are much higher than on the rest of the DU.

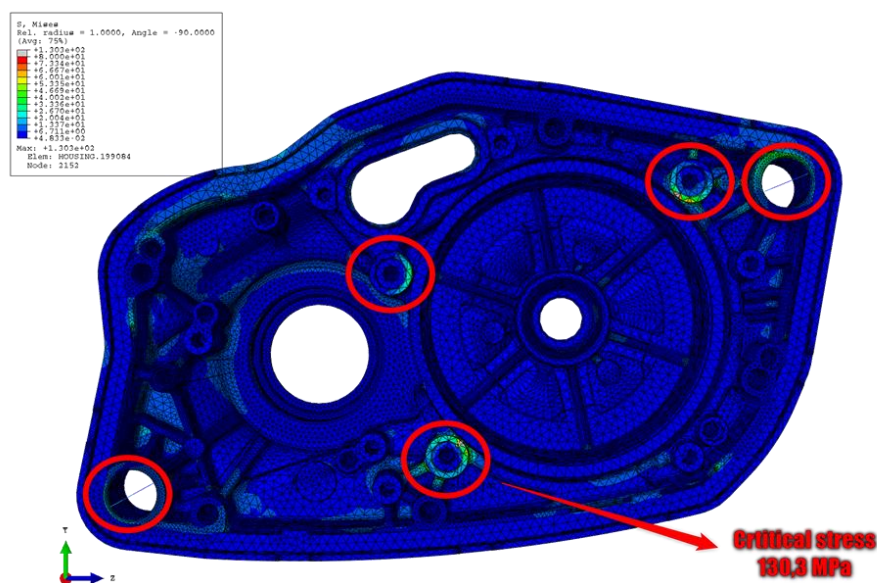


Figure 31. Simulation results for the angle of 135 degrees (BCs areas circle in red)

In fact, far from the boundary condition areas, the stresses on the rest of the DU for this pedal angle do not exceed 40 MPa. The stress singularities introduce here an error of approximately 325% in this case. It is therefore necessary to carefully integrate them into the following analysis: by moving away from boundary conditions areas when analyzing stresses. To avoid these singularities, for the remainder of the analysis, stresses exceeding 80 MPa will not be included in the legend scale; these areas will be shaded on the DU model. According to tests conducted by BOSCH under real-world operating conditions for the DU, the mechanical stress does not exceed 80 MPa; this limit therefore allows for the isolation of the effects of stress singularities. Furthermore, the yield strength of the DU material (magnesium) is 140 MPa, so this 80 MPa limit is well below the critical stress.

4.1.3.2 Results

Within the scope of this study, the analysis of the DU's mechanical stress is limited solely to that of the cover/housing assembly. The results of the simulation are shown in Figure 32:

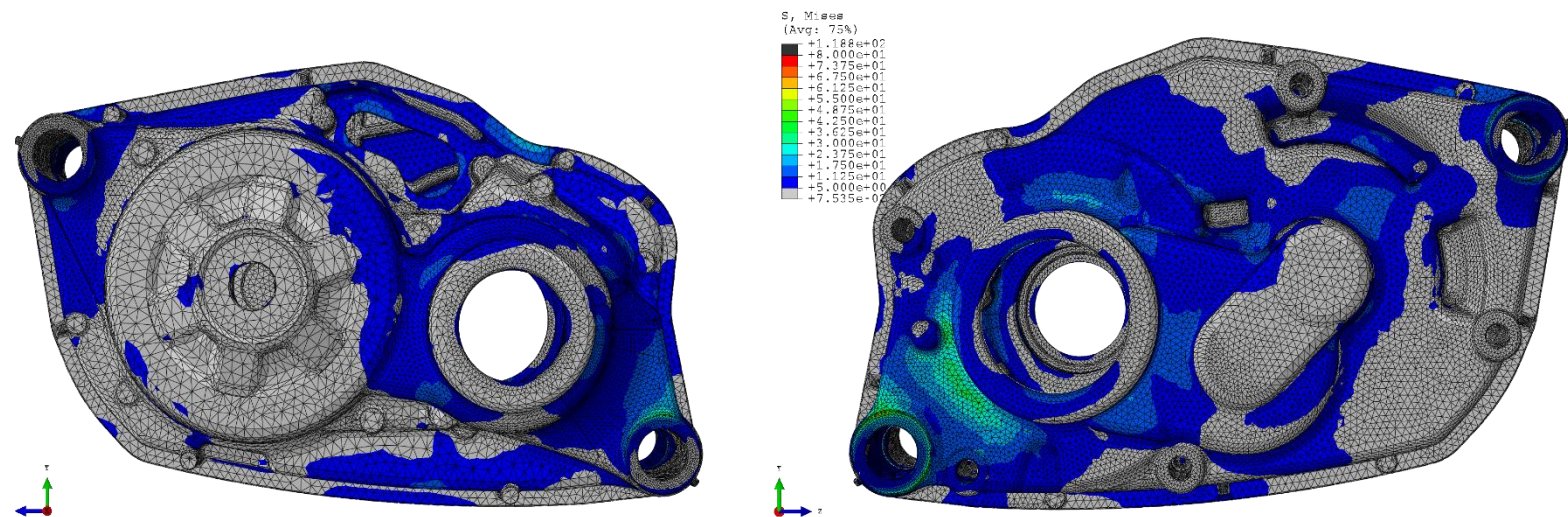


Figure 32. DU simulation results (90 degrees)

After addressing the topic of stress singularities, it is now possible to correctly analyze the simulation results for the selected dataset. To do this, it was necessary to observe the stress states of the BDU stage for each of the simulation steps. It was therefore possible to isolate the most restrictive case for the DU. In addition, the stress scale has been modified to exclude stress singularities and provide a clearer representation of the stress distribution in the DU (see above Figure 32). In fact, the light gray areas represent zones subjected to stresses below 5 MPa (negligible), while the dark gray/black areas represent zones where the mechanical stress exceeds the scale limit, in this case, 80 MPa. Here, the light gray areas (< 5 MPa) are predominant; the few dark gray/black areas are located within the DU in the regions where attachments are present (see Figure 31).

Then, the critical angle for this situation is 90 degrees, for this step, the maximal stress experienced by the DU does not exceed 48 MPa. This is quite consistent, since it corresponds to the angle at which maximum force is applied on the pedals. The stresses induced by the electric assistance have not changed the value of the critical angle of the DU here. Moreover, the DU stays largely in the elastic zone as long as the maximal elastic constraint of the DU is around 140 MPa (material data). It is also reassuring because the test is carried out under fairly basic conditions. Around the central circular openings (where the drive crankshaft passes through), the stresses are also higher, particularly on the right side of the DU: the side where the maximum force component is applied. Finally, the drive unit does not allow for different critical angles for each side of the housing: both the cover (right) and the housing (left side) experience maximum stress for this critical angle of 90 degrees.

To get a more accurate idea of the effect of electric assistance on the stress state of the BDU, the next section will present the results of the same simulation, but this time without electric assistance.

4.1.4 Electric assistance off

The results of the simulation can be seen in Figure 33:

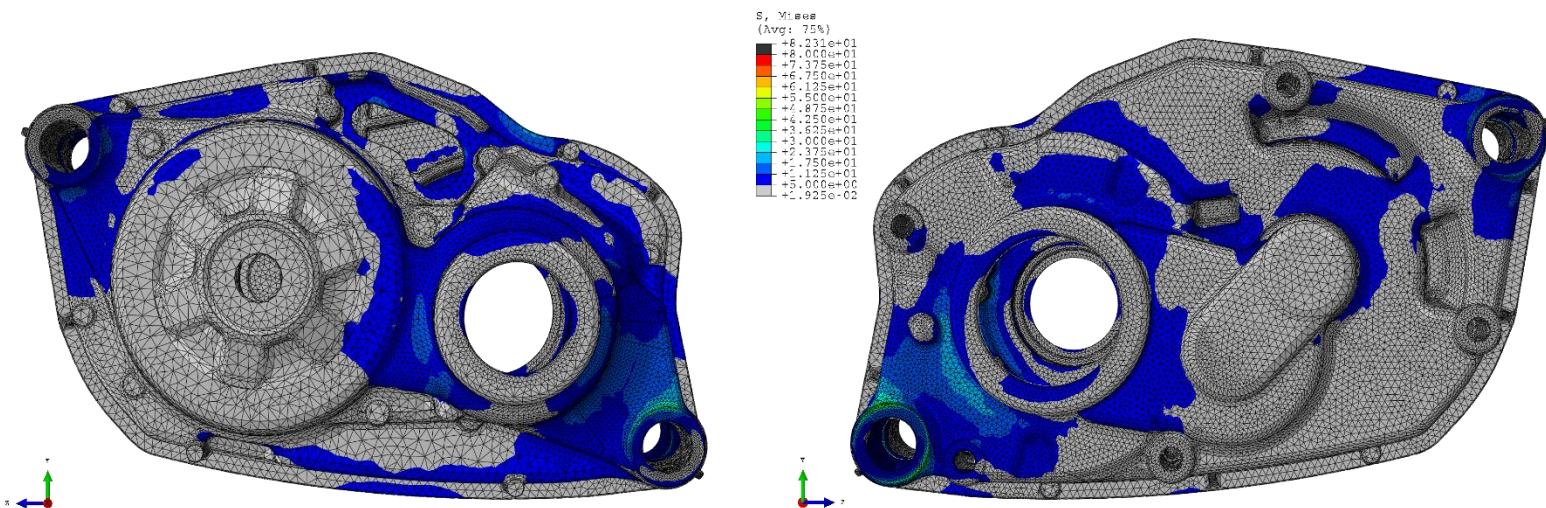


Figure 33. DU simulation results without electric assistance (90 degrees)

First, the critical angle of the simulation remains the same despite the deactivation of the electric assistance. Then, it is easily noticeable that the DU is subject to less mechanical stress as they are fewer blue zones: it means that a greater part of the DU is subjected to stress not exceeding 5 MPa, compared to the previous case. The green zones are also smaller and clearer, indicating a smaller maximum constraint, indeed, the maximum constraint does not exceed 30 MPa. This corresponds to an increase of approximately 60% in the maximum stress for the case with the electric assistance on.

This increase in maximum stress for the case including electric assistance fully justifies the analysis with and without assistance, as the internal forces generated by the motor are a significant factor in the stress on the casing. However, the maximum stress observed in the worst-case scenario (with assistance) represents approximately 34% of the elastic limit. This indicates a very large safety margin regarding plastic deformation under static load conditions. The casing is far from its static breaking limit. There is no risk of damages under these loads.

4.2 ISO norm test comparison

In fact, the mechanical stress test generally used by the DU testing team is the ISO standard norm test, which is overly conservative in order to guarantee a certain level of resistance for the crankshaft and therefore good safety for the user. It is different from the test developed in this study, and it is therefore relevant to compare them. This section will begin with a brief description of the ISO standard test before moving on to a comparison of the two tests.

4.2.1 ISO norm test

ISO standards serve as internationally recognized benchmarks and guidelines designed to ensure that products, services, and systems are safe, reliable, and of good quality. They are developed through a consensus-based process involving experts from around the world. A special experience has been designed for this case of drive unit test.

This test aims to simulate conservative pedal forces, the entire drivetrain is prevented from rotating, and embedded on a rigid testing rig. The chain force counteracts the crankshaft: the configuration of the test is similar to the one used in the study. This test consists in applying the same vertical force successively to each crank arm (drive side crank and non-drive side crank), which are specifically positioned at a 45° angle relative to the horizontal. The test configuration is detailed in Figure 34 [6]:

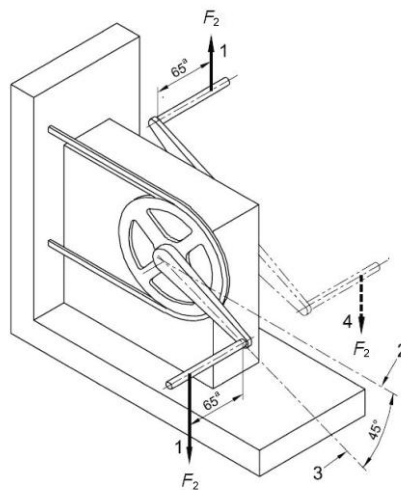


Figure 34. Crank unit: ISO test with crank arms inclined at 45 degrees to the horizontal (typical test setup)

With:

1. The repeatedly applied test force
2. The horizontal axis
3. The crank axle or axis
4. The alternative arrangement of the non-drive-side crank
 - a from the outer surface of the crank arm

Moreover:

$$F_2 = 1800 \text{ N} \quad (16)$$

So, the simulation of this test then contains two steps, one with the force F_2 on the drive side crank positioned at 45 degrees, and another one with the same force on the non-drive side crank positioned at 45 degrees. The next section will then be devoted to comparing these results with the results of the study simulation for the critical angle.

4.2.2 Comparison and use of a scale factor

The forces applying for the ISO norm test are significantly higher than the one applied in the pedaling cycle simulation previously realized. Consequently, to perform relevant comparison and analyses, the pedaling cycle data at the critical angle (90 degrees) will be scaled to reach the same maximum pedal force: 1800N. The electric assistance will also be increased to its maximum level; thus, the electric assistance induced the maximum mechanical stress also. The comparison will therefore be made between the stress state of the DU for the critical angle of 90 degrees, under the same pedaling cycle with modified values (scaled up), and between the stress states of the two loading states of the ISO standard.

Thus, the pedaling forces and the motor moment applied on the DU simulation model for the non-ISO simulation will be scaled up (forces multiplied by ca. 2.7 and motor torque by 2) and compiled in Table 1:

Table 1. Scaled pedaling cycle data for the critical angle (90 degrees)

Motor torque [Nm]	FXL [N]	FXR [N]	FYL [N]	FYR [N]	FZL [N]	FZR [N]
4.08	-354.7	131.92	-404.24	-1800.26	127.68	-236.03

It should be noted that the critical angle of the pedaling cycle originally chosen for this study is relatively close to the pedal angle established in the ISO standard tests. It is therefore considered relevant to compare these two tests.

DU scaled simulation:

The resulting stress state of the DU can be observed in Figure 35:

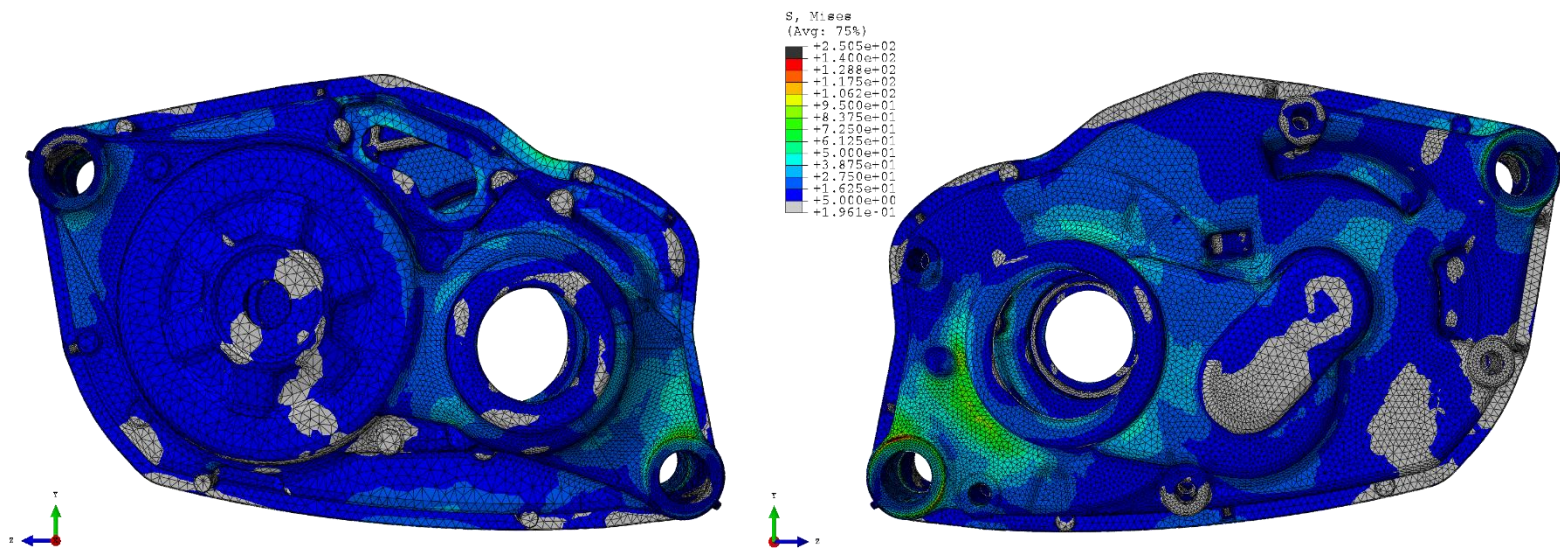


Figure 35. DU scaled simulation results (90 degrees)

Now, almost all the DU experiences a Mises constraint of at least 5 MPa. The most important mechanical stresses remain around the zones where the crankshaft is mounted. However, apart from this area, the casing constraint rarely exceeds 50 MPa. Away from the boundary conditions, the maximal stress reaches the 95 MPa, which is still quite far from the maximum elastic limit of the motor. But, in the zones of the fastening screws (see figure 9 in the section [Boundary conditions](#)), which attach the DU to the fictional frame, especially the ones at the bottom, Abaqus displays a resulting stress of 250MPa: theoretically exceeding the elastic limit. It is difficult to give an analysis of the result in these zones, as long as they correspond to boundary conditions zones, so stress singularities make the Mises stress difficult to interpret. In the reality, the maximum stress in these zones do not exceed 250MPa, but it is difficult to state if the casing is experiencing damages.

It is difficult to perform a realistic analysis of this stress state under the condition of this study. A real-world experiment could have clarified these results, but this was not within the scope of this work. However, the ISO standard tests were tested by BOSCH eBike on test benches. So, the comparison with the ISO norm test will enable to highlight the influence of the triaxiality of the pedal forces and the influence of the electric assistance on the stress state of the DU.

ISO norm test simulation:

The both resulting stress states of the DU can be observed in Figures 36 and 37:

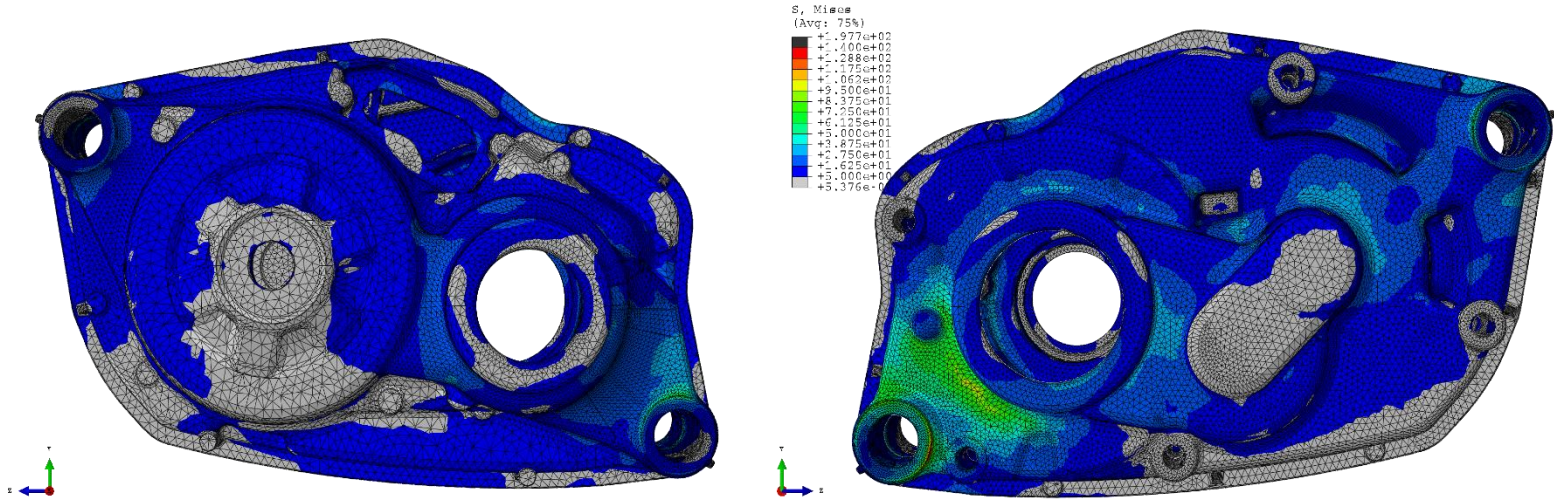


Figure 36. ISO norm test simulation results: drive side crank

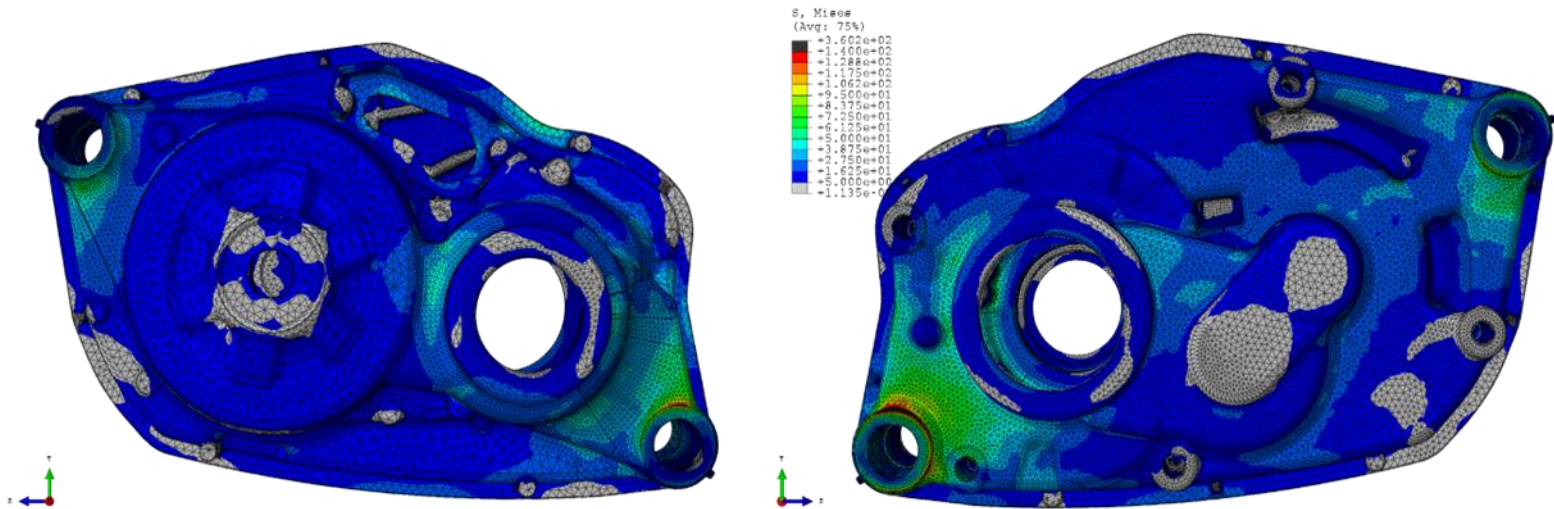


Figure 37. ISO norm test simulation results: non-drive side crank

The ISO drive side crank test is generally less demanding for the casing. Indeed, a larger part of the motor is experiencing a stress lower than 5MPa , blue and light blue zones are less extended. Apart from the stress singularities zones, the maximum stress is the same than in the previous test and the corresponding zone is also the same for the DU. However, including the stress singularities zone, the maximum stress is lower than in the previous test, but it concerns also the same zone. This test corresponds to the pedal force applied on the right side of the DU: force applied on the same side than the previous test.

Regarding the ISO non-drive side, the DU is experiencing slightly higher stress compared to the other side: more zones exceed a stress of 5MPa or more. Areas exceeding 5MPa are consistent with those observed for the scale cycle test. The

maximum stress (ca. 95MPa) is located near the bottom fixation screws, near the BCs, compared to the two other tests, where it is more around the crankshaft bearing area in the casing. The overall stress level is not significantly different from the one of the tests with the scale pedaling cycle. However, in the stress singularities zones, especially the bottom fastening screws, the von Mises constraint is largely higher than in the two other tests (ca. 360MPa compared to 197.7MPa and 250.5MPa). Due to these stress singularities, it is not possible to draw conclusions about real von Mises stress values. However, real ISO standard tests conducted by BOSCH have proven that these areas are indeed the most stressed during testing and that, despite very high pedal forces, the DU remains within the elastic range. Furthermore, the ISO test (non-drive side step) remains the most conservative and demanding test for the casing, even though it does not include any triaxial pedal forces and electric assistance induced forces. It can therefore be concluded that, during the scaled pedaling cycle test, the DU is under high stress, but it also remains within the elastic range. Finally, a slight difference in stresses in the shafts attachment areas in the motor is visible between the scaled test and the ISO standard tests. The electric assistance induced forces produce greater stresses on the DU in these areas, but these stresses remain low compared to the elastic limit of the DU material. These attachment zones are highlighted in Figure 38:

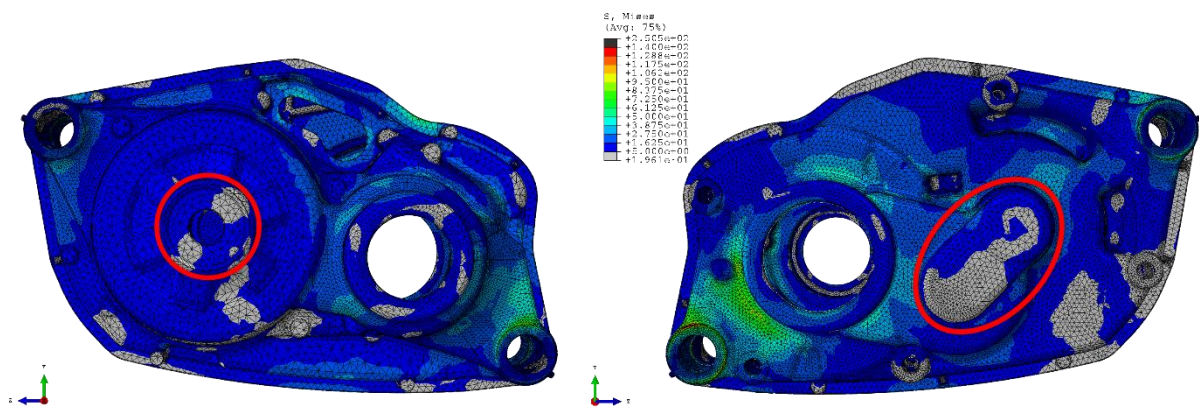


Figure 38. Shafts attachment areas in the DU (scaled pedaling cycle test results)

In conclusion, while the scaled pedaling cycle test incorporates electric assistance and triaxial forces that are absent in the ISO standard tests, these additional forces, although they increase the stresses in the shaft attachment areas, keep the drive unit below its elastic limit. Despite the absence of these real-world stress components, the ISO non-drive side test remains the most conservative and demanding assessment for the casing. This is because, even without electric assistance and triaxial forces, it generates significantly higher stress concentrations, particularly around the bottom fastening screws, which are proven to be the most stressed areas. Crucially, even under these extreme conditions, the DU consistently remains within its elastic range, demonstrating its robust design. Therefore, although the scaled test offers a more comprehensive

simulation of actual riding conditions, the ISO non-drive side test's high-stress application, leading to the DU's elastic response, ultimately makes it strictest and the most conservative benchmark for assessing structural integrity.

4.3 Workflow documentation – Knowledge transfer

The aim of this master thesis was to develop an automated working method that could be adapted to other BOSCH eBike products, which was easy to use, and could subsequently be reused by the DU simulation teams.

To facilitate these last requirements, a comprehensive knowledge transfer is necessary. As a result, a complete and detailed folder will be compiled and submitted to the eBike DU simulation team. This extensive document will serve as a centralized repository for all digital tools developed, adapted, and employed during the research study:

- FEM DU simulation model
- Bearing reaction forces calculation Excel sheet
- Python automation script
- Shell automation script

Each component will be annotated, providing clear and accurate explanations of its purpose, highlighting principles, and operational mechanics. This detailed explanation aims to ensure a smooth and accurate transfer, in order to avoid any potential loss of knowledge. The goal is to enable future team members or researchers who take over this work to quickly understand the methodologies and technical aspects, facilitating comprehension and practical application. In addition to this dossier, a comprehensive report will be written, detailing specific step-by-step instructions for the use, configuration, and troubleshooting of each of these documented tools.

5. Conclusions

This study enabled the successful development and implementation of a new automated workflow for analysing stress states inside the drive unit casing of an electric bicycle motor under realistic pedaling conditions, integrating electric assistance and triaxial pedaling forces. By going beyond traditional static or simplified load conditions, this approach provides a better understanding of the structural response of the DU, through a real pedaling cycle. The developed process, which encompasses the processing of actual load cycle data, finite element analysis using Abaqus, and significant automation via Python and Shell scripts, enables the effective identification of critical stress areas throughout a complete pedaling cycle.

An important conclusion is the significant influence of electric assistance on the stresses exerted on the DU, during a standard pedaling cycle at average pedaling forces. Simulations revealed that electric assistance induces maximum stresses approximately 60% higher in the casing compared to scenarios without assistance. Despite this increase, the maximum stresses observed, even in the worst-case scenarios, remained well below the elastic limit of the material, indicating a significant margin of safety against plastic deformation under static loads. Thus, in absolute terms, this increase is significant, but in the context of the static load limit, this increase is not sufficient to make the motor's mechanical stresses critical. On the other hand, the important challenge or difference will probably be encountered in terms of fatigue resistance over a large number of load cycles, rather than in terms of the risk of breakage or plastic deformation under maximum instantaneous loads.

In addition, a critical comparison was made between the realistic pedaling cycle test developed and existing ISO standard tests. While the scaled pedaling cycle test incorporates more realistic elements such as triaxial forces on the pedals and electric assistance, the ISO test was identified as the most conservative and demanding assessment for the DU housing (especially, non-drive side test step). This is due to the presence of significantly higher localized stress concentrations, particularly around the lower mounting screws. It is important to note that even under these extreme ISO test conditions, and despite the simplified application of loads (no triaxial forces and no electric assistance), the DU consistently demonstrated robust performance, remaining within its elastic range (according to BOSCH real test results). The contribution of triaxial forces and electrical assistance, although present in real-world scenarios and captured by the scaled-up test, proved less demanding for the DU compared to the stress levels imposed by the ISO standard, in the scope of this study.

Finally, one of the significant results of this thesis is the creation of a fully documented and automated workflow that is easily adaptable and transferable to other BOSCH

electric motors, ensuring continuity of knowledge and improving future simulation capabilities within the DU simulation team.

6. Points of perspective

This study has successfully developed a broader methodology for assessing the stresses within eBike motors. However, like any research, it naturally highlights avenues for further exploration and refinement.

Concerning pedaling data, it would have been a good idea to test and analyse the mechanical strength of the DU under various types of cycles: uphill slopes, with heavyweight cyclists, irregular terrains, etc. In addition, the refinement of the data, such as taking a smaller sampling rate or refine the dataset around the critical angles, would have given more accurate results about the DU.

In terms of simulation, Abaqus results would be of better quality, if the mesh of the electric motor was more refined: the mapping of the critical stresses area would be more precise. Moreover, a refined mesh combined to a nonlinear finite element model of the DU would avoid the stress singularities on the simulation results. Thus, Abaqus FEM results would be more reliable, and it would be easier to evaluate the elastic response of the DU.

While this study focused on static stress analysis, the observation that electric assistance increases maximum stresses suggests a potential impact on fatigue life. Future work should also integrate the developed workflow with fatigue analysis methods to predict the long-term durability of the DU under a large number of load cycles, considering the dynamic nature of both pedaling and motor assistance.

Then, for this study, two programming languages were used to fully automate the developed working method: Python and Shell. However, it would be interesting to explore the possibilities of processing everything with the Python language. This could potentially further reduce the number of manual intermediate steps in the working method, allowing engineers to save even more time.

Also, adding an experimental validation step to the working method would make it possible to verify the results obtained during the simulation, thereby making the working method complete and more reliable.

Finally, it would be appropriate to broaden the scope of the study further by including the environmental component: attempting to carry out a strength analysis of DU using several materials, particularly more environmentally friendly materials. Currently, the DU is made of magnesium, which is lightweight but has a considerable environmental impact.

References

- [1] “BOSCH - Our history,” Bosch Global. Accessed: Mar. 28, 2026. [Online]. Available: <https://www.bosch.com/company/our-history/>
- [2] Ernst Brust, “Marktanalyse der Pedelec-Motorenhersteller in Deutschland, Europa und weltweit,” *VeloTOTAL - Aktuelles zum Radfahren*, Nov. 04, 2024. Accessed: Jan. 23, 2026. [Online]. Available: <http://www.velototal.de/2024/11/04/marktanalyse-der-pedelec-motorenhersteller-in-deutschland-europa-und-weltweit/>
- [3] H. Ritchie and M. Roser, “CO₂ emissions,” *Our World in Data*, Jun. 2020, Accessed: Mar. 28, 2026. [Online]. Available: <https://ourworldindata.org/co2-emissions>
- [4] “Planetary boundaries.” Accessed: Mar. 28, 2026. [Online]. Available: <https://www.stockholmresilience.org/research/planetary-boundaries.html>
- [5] H. Ritchie, “Cars, planes, trains: where do CO₂ emissions from transport come from?,” *Our World in Data*, Oct. 2020, Accessed: Jan. 23, 2026. [Online]. Available: <https://ourworldindata.org/co2-emissions-from-transport>
- [6] DIN Deutsches Institut für Normung e. V, “Cycles –Safety requirements for bicycles – Part 8: Pedal and drive system test methods ISO 4210-8:2014.” Jan. 2015.
- [7] M. Steck, “Robust service life-oriented simulation method to support the design of eBike Drive Units,” Doktoringenieur Thesis, Technischen Universität Ilmenau, 2025.
- [8] I. Malick, “Modélisation mécanique et étude de la rigidité de la Drive Unit,” Grenoble INP - ENSE3, Thèse de Master, Sep. 2025.
- [9] F. L. Litvin and A. Fuentes, Eds., “Involute Helical Gears with Parallel Axes,” in *Gear Geometry and Applied Theory*, 2nd ed., Cambridge: Cambridge University Press, 2004, pp. 375–403. doi: 10.1017/CBO9780511547126.016.
- [10] Y. Li, R. Huang, S. Zhao, and J. Wang, “Contact pressure analysis of pin-loaded lug with clearance,” *Advances in Mechanical Engineering*, vol. 14, no. 6, Jun. 2022, doi: 10.1177/16878132221107475.
- [11] M. Aublin, R. Boncompain, and M. Boulaton, *Systèmes mécaniques: théorie et dimensionnement*. Dunod, 1993.
- [12] D. Spenlé and R. Gourhant, *Guide du calcul en mécanique: maîtriser la performance des systèmes industriels*. Hachette technique, 2003.
- [13] R. v. Mises, “Mechanik der festen Körper im plastisch- deformablen Zustand,” *Nachrichten von der Gesellschaft der Wissenschaften zu Göttingen, Mathematisch-Physikalische Klasse*, vol. 1913, pp. 582–592, 1913.
- [14] D. L. Logan, *A First Course in the Finite Element Method, SI Version*. Cengage Learning, 2011.
- [15] D. S. DUGDALE, “CHAPTER 4 - PLANE STRESS AND STRAIN,” in *Elements of Elasticity*, D. S. DUGDALE, Ed., in The Commonwealth and International Library: Structures and Solid Body Mechanics Division. , Pergamon, 1968, pp. 41–55. doi: <https://doi.org/10.1016/B978-0-08-203495-7.50007-8>.
- [16] K. J. Bathe, *Finite Element Procedures*. Prentice Hall, 2006.
- [17] R. M. Andrew and G. P. Peters, “The Global Carbon Project’s fossil CO₂ emissions dataset (2025v15).” 2025. doi: <https://doi.org/10.5281/zenodo.17417124>.

Appendix

Appendix 1

The evolution of the worldwide annual CO₂ emissions from 1750 to these days is summarized in the Figure A-1, based on data from “The Global Carbon Project’s fossil CO₂ emissions dataset” [17].

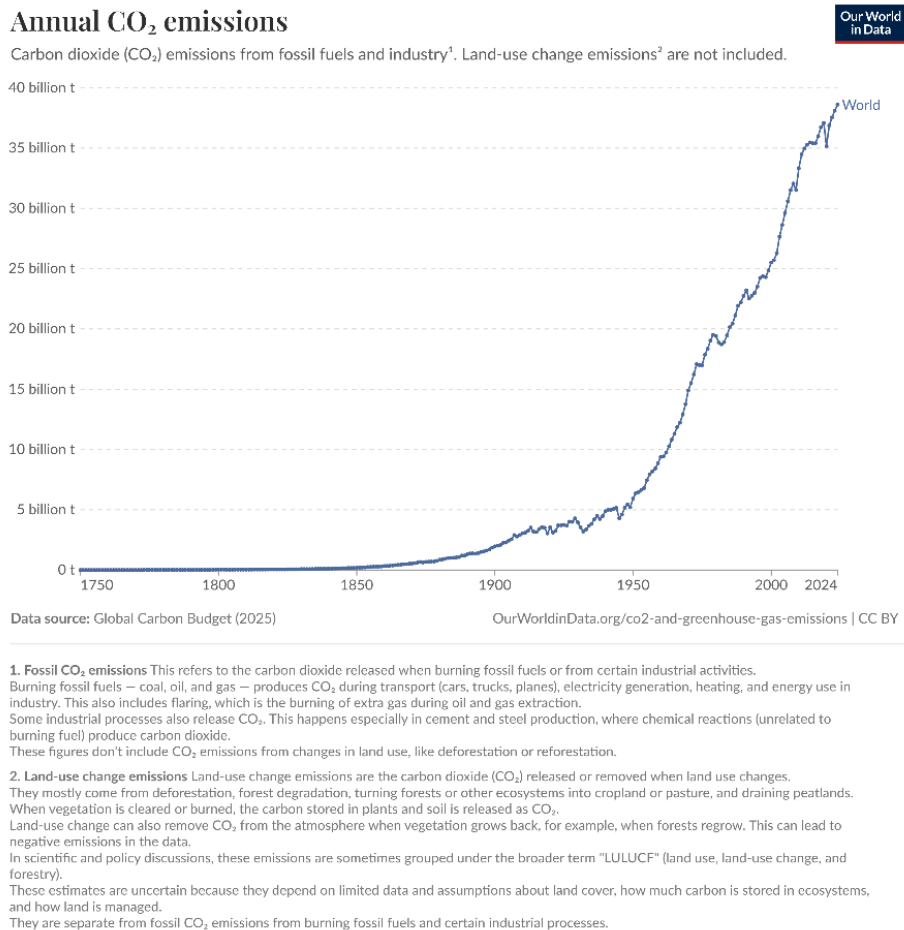


Figure A- 1. Annual CO₂ emissions based on [17]

Appendix 2

Figure A-2 represents the different planetary boundaries and their exceedance in 2025, based on analysis in Sakschewski and Caesar et al. 2025 [4].

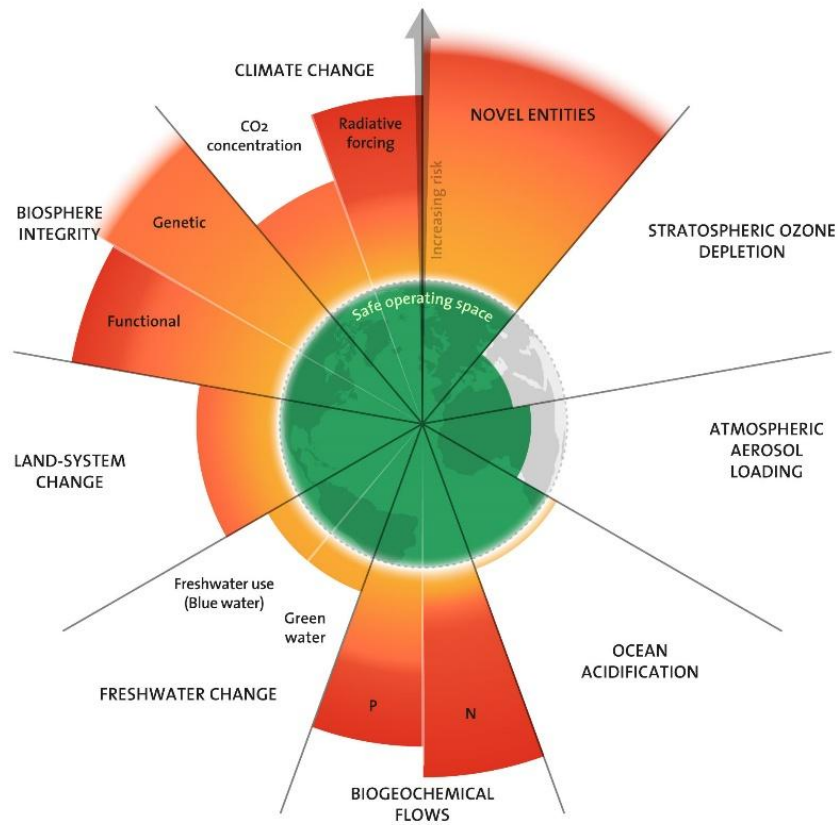


Figure A- 2. The 2025 update to the Planetary boundaries

Appendix 3

The first part of an example of a FORTRAN subroutine script used for the thesis work is detailed in Figure A-3.

```
Subroutine appendix
1 SUBROUTINE DLOAD(F,KSTEP,KINC,TIME,NOEL,NPT,LAYER,KSPT, &
2 COORDS,JLTYP,SNAME)
3
4 INCLUDE 'ABA_PARAM.INC'
5
6 DIMENSION TIME(2), COORDS(3)
7 CHARACTER*80 SNAME
8
9 ! Spatial coordinate system
10 x = COORDS(1) ! axial
11 y = COORDS(2) ! vertical
12 z = COORDS(3) ! horizontal
13
14 ! DLOAD parameters
15 pi = 3.14159265359
16 theta0 = pi/2
17
18 ! Bearing forces [N]
19 ! Initialize with default values
20 Fy = 0.0
21 Fz = 0.0
22
23 if (KSTEP==1) then
24     u=0+TIME(1) ! ramp for load application
25 endif
26
27 ! --- Conditional forces and parameters based on SNAME ---
28 IF (SNAME .EQ. 'ASSEMBLY_LAGER-L1-1_IN') THEN
29     bearing_x = 46
30     bearing_y = 0
31     bearing_z = 0
32     Fy = 4000
33     Fz = 4000
34     d = 31.0 ! bearing diameter
35     b = 8.5 ! bearing width
36 ELSE IF (SNAME .EQ. 'ASSEMBLY_LAGER-L3-1_IN') THEN
37     ...
38 END IF
39 ! -----
40
41 ! Initialize F
42 F = 0.0
43
44 ! Calculate relative position from bearing center
45 rel_y = y - bearing_y
46 rel_z = z - bearing_z
47
48 ! Applying pressure profile
49 FB = sqrt(Fy**2 + Fz**2)*u
50 phiFB = atan2(Fz, Fy)
51 theta = atan2(rel_z, rel_y)
52 Pmax = 4.0/pi * FB/(d*b)
53
54 if (cos(theta-phiFB) >= cos(theta0)) then
55     F = Pmax * cos(theta-phiFB)
56 endif
57
58 RETURN
59 END SUBROUTINE DLOAD
60
61 SUBROUTINE UTRACLOAD(ALPHA,T_USER,KSTEP,KINC,TIME,NOEL,NPT, &
62 COORDS,DIRCOS,JLTYP,SNAME)
63
64 INCLUDE 'ABA_PARAM.INC'
65
66 DIMENSION T_USER(3), TIME(2), COORDS(3), DIRCOS(3,3)
67 CHARACTER*80 SNAME
68
69 ! Spatial coordinate system
70 x = COORDS(1) ! axial
71 y = COORDS(2) ! vertical
72 z = COORDS(3) ! horizontal
73
```

Figure A- 3. FORTRAN subroutine, Part 1

Appendix 4

The second part of the previous FORTRAN subroutine script used for the thesis work is detailed in Figure A-4.

```
73
74      ! DLOAD parameters
75      pi = 3.14159265359
76      theta0 = pi/2
77
78      ! Bearing forces [N] - Define all needed forces here
79      ! Initialize with default values
80      Fx = 0.0
81      Fy = 0.0
82      Fz = 0.0
83      ! Bearing parameters - Initialize with default or common values
84      d = 40.0      ! bearing diameter
85      b = 7.0      ! bearing width
86
87      if (KSTEP==1) then
88          u=0+TIME(1)      ! ramp for load application
89      endif
90
91      ! --- Conditional forces and parameters based on SNAME ---
92      IF (SNAME .EQ. 'ASSEMBLY_LAGER-L1-1_IN') THEN
93          bearing_x = 46
94          bearing_y = 0.0
95          bearing_z = 0.0
96              Fx = 4000
97              Fy = 4000
98              Fz = 4000
99              d = 31.0 ! bearing diameter
100             b = 8.5 ! bearing width
101      ELSE IF (SNAME .EQ. 'ASSEMBLY_LAGER-L3-1_IN') THEN
102          ...
103      END IF
104      ! -----
105
106      ! Initialize variables
107      ALPHA = 0.0
108      T_USER = [0.0, 0.0, 0.0]
109
110      ! Calculate relative position
111      rel_y = y - bearing_y
112      rel_z = z - bearing_z
113
114      phiFB = atan2(Fz, Fy)
115      theta = atan2(rel_z, rel_y)
116
117      if (Fx < 0) then
118          T_USER = [-1.0, 0.0, 0.0]
119          FB = -Fx
120      else
121          T_USER = [1.0, 0.0, 0.0]
122          FB = Fx
123      endif
124
125      if (cos(theta-phiFB) >= cos(theta0)) then
126          ALPHA = FB/(theta0*d*b)*u
127      else
128          ALPHA = 0.0
129      endif
130
131      RETURN
132  END SUBROUTINE UTRACLOAD
```

Figure A- 4. FORTRAN subroutine, Part 2

